A General Circulation Model of a Venus-Like Atmosphere

WILLIAM B. ROSSOW

NASA/Goddard Space Flight Center, Institute for Space Studies, New York, NY 10025

(Manuscript received 18 January 1982, in final form 26 August 1982)

ABSTRACT

A three-dimensional general circulation model of a slowly rotating, massive atmosphere is forced with an axisymmetric radiative heating/cooling distribution to explore the heat and momentum budgets established in this type of atmosphere. In the model lower atmosphere, the mean meridional circulation, as suggested by Stone (1974), balances the differential radiative heating and maintains a statically stable, quasi-barotropic thermal state. However, the nature of this balance depends crucially on the momentum budget established. Although small-scale convection and eddies also play a role in maintaining the static stability of the lower atmosphere, eddy horizontal heat transport is completely negligible. The meridional circulation takes the form of multiple equator-to-pole cells, one above the other. The correlation of this vertical structure with the vertical distribution of radiative and convective/eddy heating suggests that the net heating vertical distribution produces this multicellular structure. The model results confirm the proposals of Gierasch (1975) and Rossow and Williams (1979) in a fully three-dimensional circulation. The mean meridional circulation, despite its multicellular form, interacts with quasi-barotropic eddies produced by zonal flow shear instability to produce a weak superrotation of the entire model atmosphere. This process is general enough to conclude that it will occur in all slowly rotating atmospheres; but, whether it can accelerate wind speeds as large as those observed on Venus, cannot be determined yet.

1. Introduction

The slow rotation of Venus places its atmospheric dynamics outside of the familiar regime of quasi-geostrophic motions which have been the focus of most atmospheric studies. Although some qualitative discussion of this dynamical regime has occurred, based on simplified linear or one- and two-dimensional models and on laboratory experiments, little exploration of nonlinear, three-dimensional general circulations on slowly rotating spheres has been done. Recent spacecraft observations have begun the task of describing the properties of the Venus atmosphere and circulation, but these data are not adequate to guide exploration of this dynamic regime because they do not even define the basic circulation of the bulk of the atmosphere. Consequently, modeling studies must be considered explorations of the processes that *might* be important to the general circulation of slowly rotating atmospheres and, possibly, Venus. Whether a particular process is important in a particular atmosphere, such asVenus, probably depends on details of atmospheric physics which are not yet available from observations; however, examination of model behavior can be instructive in two ways. 1) If the model dynamics are general enough, then the dynamical processes which can be examined in the model should be present, though not necessarily dominant, in *all* slowly rotating atmospheres. This does not preclude the existence of other processes which do not occur in the model, however. 2) Comparison of differences and similarities between model behavior and Venus observations can suggest questions for further model study and interpretations of the observations to be verified by further measurements. In this fashion, the model results discussed in this paper are not intended to represent a simulation of Venus, but rather an exploration of the slowly rotating dynamic regime. Understanding Venus, however, does provide the motivation for such an exploration.

Study of the slowly rotating dynamic regime has generally been a study of Venus' general circulation. These theoretical investigations have focused on two fundamental problems. One problem concerns the organization of the atmospheric circulation on a slowly rotating planet to accomplish the heat transport required by differential solar heating. The expectation is that a Hadley-like circulation will predominate with small- and large-scale eddies largely absent, as observed in laboratory experiments (Fultz *et al.*, 1959; Spence and Fultz, 1977); but if radiative heating produces large temperature contrasts in Venus' massive lower atmosphere, they might force other dynamic modes of heat transport which could replace all or part of the heat transport by the mean meridional flow. The second problem concerns the nature of the momentum transport processes in Venus' atmosphere, especially those that produce a large, but weakly divergent, zonal flow in the cloud-filled upper

atmosphere. Two alternatives have been proposed, either upward momentum transport by propagating wave modes predominates (Schubert and Whitehead, 1969; Fels and Lindzen, 1974) or that by the mean meridional circulation does (Gierasch, 1975). Neither of these processes has been investigated in a three-dimensional circulation, however. In Section 2, a brief review of previous work on these two general problems leads to four particular questions which are the focus of this model investigation. 1) Can the mean meridional circulation provide the dominant vertical and horizontal heat flux in a massive, slowly rotating atmosphere as suggested by Stone (1974) and others? 2) What determines the vertical and horizontal structure of the mean meridional circulation? 3) Can the mean meridional circulation transport momentum over large vertical distances as suggested by Gierasch (1975)? 4) Do some eddy motions behave as if they were barotropic, two-dimensional motions as suggested by Rossow and Williams (1979)?

The model used for this investigation is a version of the GFDL[1] 9-level, 15-wavenumber spectral general circulation model of Earth's atmosphere, modified to resemble Venus, as described in Section 3. The full generality of the equations of motion is retained, but the model physics have been simplified to isolate particular regimes or processes. First, to study the relative importance of the mean meridional circulation and small-scale convection for maintaining the static stability in the lower atmosphere, the vertical profile of net radiative heating is chosen to produce a large (superadiabatic) temperature lapse rate in the lower atmosphere, and a small (subadiabatic) lapse rate in the upper atmosphere. Second, a simple latitudinal variation of net radiative heating is chosen to exaggerate the equator-to-pole temperature gradient. Both of these choices are directed towards stimulating other modes of heat transport in competition with the mean meridional circulation. Third, the net radiative heating is taken to be axisymmetric to remove any *explicit* forcing of propagating wave modes, particularly in the upper atmosphere, and to isolate vertical momentum transport by the mean meridional circulation. This choice deliberately removes the so-called "moving flame" mechanism in order to study the mechanism proposed by Gierasch (1975). The calculation is started from an initially motionless and isothermal state; the resulting equilibrium circulation is described in Section 4.

The diagnosis of the model circulation in Section 4 serves as a basis for discussing, in Section 5, the four questions mentioned above and developed in Section 2. The detailed examination of the model's heat and momentum budgets, together with a description of the eddy motions, suggests preliminary answers to these questions in that the model is one realization of a slowly rotating atmosphere. Observations of Venus, which is another realization, are also considered for their implications regarding these same issues. This discussion is summarized in Section 6.

2. Theoretical problems with Venus' atmosphere[2]

a. Why is the surface so hot?

The surface temperature of Venus is more than twice that of Earth despite absorbing only half as much solar energy (Tomasko *et al.*, 1980b), so that consideration of the heat budget has focused primarily on explaining this fact. Recent spacecraft observations, especially from Pioneer Venus, strongly support the "greenhouse" explanation (Sagan, 1962; Pollack, 1969) because they show that $\sim$10% of the total absorbed sunlight reaches the surface (Tomasko *et al.*, 1980a) and that the atmosphere appears to have sufficient infrared opacity to produce the high surface temperature radiatively (Pollack *et al.*, 1980; Tomasko *et al.*, 1980b). Goody and Robinson (1966) proposed an alternative dynamical explanation for the high surface temperature; but Kalnay de Rivas (1973, 1975) showed that density stratification effects, which were neglected by Goody and Robinson, confine the thermally forced, *mean* meridional circulation to the cloud levels unless a substantial fraction of the total solar energy is absorbed at deeper levels. Although the high surface temperature appears explainable as a radiative process, the work of Kalnay de Rivas and others raises several key questions concerning the form of the thermally driven circulation and the role of that circulation in the heat budget of Venus' atmosphere.

Calculations of the radiative equilibrium temperature structure produce superadiabatic profiles in the lower atmosphere (Pollack and Young, 1975; Pollack *et al.*, 1980), which require some dynamic vertical heat flux to maintain the observed, nearly neutral stability (Marov, 1978). The usual assumption in this case is that small-scale convection maintains an adiabatic lapse rate and provides the bulk of the dynamic vertical heat flux; but scale analyses of Hadley circulations (Gierasch *et al.*, 1970; Stone, 1974) suggest that these large-scale circulations, driven by horizontal heating contrasts, can also provide the necessary vertical heat flux to maintain an adiabatic lapse rate. Numerical, but two-dimensional, calculations also confirm this result (Kalnay de Rivas, 1975). Pioneer Venus results are not accurate enough to measure the dynamic vertical heat fluxes (Tomasko *et al.*, 1980b), and model calculations with both small-scale convection and three-dimensional large-scale motions have not been performed. Thus, the nature of the

[1] NOAA/Geophysical Fluid Dynamics Laboratory, Princeton.

[2] See the excellent review by Stone (1975).

dynamic *vertical* heat transport in a slowly rotating atmosphere is unknown.

Stone (1974) also studied the efficiency of a two-dimensional Hadley circulation for transporting heat *horizontally*, but did not include the effects of small-scale convection on static stability which can influence the efficiency of the Hadley transports. Although laboratory experiments (Fultz *et al.*, 1959; Spence and Fultz, 1977) suggest that horizontal heat transports by large-scale eddies are negligible in the slowly rotating regime, the efficiency of the mean circulation heat transport in fully three-dimensional flows in slowly rotating fluids with atmospheric properties has not been investigated.

The calculations of Kalnay de Rivas (1973, 1975) exhibit a dependence of the vertical structure of the mean circulation on the vertical distribution of the radiative heating/cooling assumed in her model. Her model circulations, and that presented here, are composed of *several cells*, one on top of the other and alternating their direction of flow; but the location and vertical extent of the thermally direct cell, as well as the number of other cells, appears to depend on the vertical distribution of solar energy. Pioneer Venus solar flux measurements (Tomasko *et al.*, 1980a) would therefore suggest a mean circulation consisting of two direct cells, one at the surface and one in the cloud layer with an indirect cell in between[3]; but dynamic vertical heat transport by other components of the circulation could alter this simple picture. The processes which control the vertical structure of the mean meridional circulation remain to be determined.

The direct Hadley cell obtained in Kalnay de Rivas' models covers all latitudes at a given altitude, except near the pole, where an indirect cell exists. Since the model is two-dimensional, eddy fluxes of momentum and heat have both been neglected. Consequently, the horizontal structure of the mean meridional circulation, which depends on the eddy fluxes in a fully three-dimensional flow (cf. Held and Hou, 1980; Taylor, 1980), remains to be explored for slowly rotating atmospheres.

b. What maintains atmospheric superrotation?

Most of the proposed explanations of the large zonal wind in the upper atmosphere of Venus concentrate on one of two general processes for the vertical transport of planetary angular momentum: Reynolds stresses by thermally forced eddy motions or advection by thermally forced mean circulations. However, none of the studies of these processes have been performed in three-dimensional models. Further, Pioneer Venus and Venera observations have shifted the theoretical problem from one of explaining strong zonal winds only in the upper atmosphere, to explaining the superrotation of the whole Venus atmosphere below the clouds.

The best known form of the Reynolds stress models was suggested by Schubert and Whitehead (1969) to explain laboratory experiments with mercury and, by analogy, to explain the Venus circulation; however, no calculation using this formulation of the problem has ever attained the Venus parameter regime (Stone, 1975). Furthermore, subsequent work suggests that the original interpretation of the laboratory results was in error when the observed motions were ascribed to bouyancy forces (Whitehead, 1972), and when the motions were assumed to be equilibrated (Douglas *et al.*, 1972). Nonlinear numerical calculations (Young *et al.*, 1972) agree with later experiments using water, where buoyancy forces do drive the motions (Douglas *et al.*, 1972), that the *mean* flow speed never exceeds the thermal wave phase speed *in equilibrium*, but that *transient* flow speeds can and do exceed the thermal wave speed.

There are two major difficulties in relating these laboratory and model results to the circulation on Venus. The first is that the laboratory experiments and the numerical models discussed by Stone (1975) consider viscous, incompressible fluids. The Pioneer Venus results show that the zonal flow covers at least six density scale heights (Counselman, *et al.*, 1980), so that the representation of vertical eddy *momentum* transports in an inviscid, compressible atmosphere by a viscous diffusion of wind speed in the equations of motion is suspect. Part of this problem is alleviated by formulating the Reynolds stresses in terms of explicit, vertically propagating wave modes and the viscous stresses as transporting wind *momentum* (cf. Fels and Lindzen, 1974). However, the eddies that are responsible for the viscous stress still seem *ad hoc* in these models, since no explicit process is proposed to explain their presence, and they are not clearly separated in length scale from the explicitly forced eddies which are held responsible for the Reynolds stresses.

The second difficulty is that all of the numerical models, including those which include density stratification effects (Young and Schubert, 1973; Fels and Lindzen, 1974; Fels, 1977), consider *local* acceleration of the zonal flow at or above cloud levels, with diffusion of momentum away from this region. The Pioneer Venus observations show that the whole atmosphere of Venus is superrotating with the angular momentum in the zonal flow concentrated at 20 km altitude and monotonically decreasing up to cloud levels and down to the surface (Schubert *et al.*, 1980). This vertical distribution of momentum strongly suggests that the primary acceleration of the flow occurs near 20 km with a weak vertical transport of mo-

[3] A direct meridional circulation is defined here to be one with poleward flow aloft and equatorward flow below. The reverse circulation is called indirect.

mentum from there into the upper atmosphere. Although the Reynolds stress of propagating waves, stimulated by diurnal heating in the clouds or near the surface (Dobrovolskis and Ingersoll, 1980), could possibly provide this weak vertical transport, no modeling studies oriented toward this role for waves have been performed. Further, since the direction and magnitude of heat and momentum transports by such propagating waves are very sensitive to the vertical temperature and wind structure, fully interactive, three-dimensional models are required to decide the role of such waves in determining the heat and momentum budgets on Venus.

The advection model (Gierasch, 1975) has vertical momentum transport to the upper atmosphere by the mean meridional circulation if some additional process of horizontal momentum transport opposes poleward advection by the meridional circulation. This additional process cannot, however, transport heat as efficiently as momentum or it will eliminate the horizontal temperature gradient which drives the meridional circulation (Kalnay de Rivas, 1975). A proposed explanation of the cause of the horizontal momentum transport and the dominance of the largest wavelength motions in the cloud top region (Travis, 1978; Rossow *et al.*, 1980; Del Genio and Rossow, 1982) is that the atmospheric circulation resembles quasi-barotropic two-dimensional turbulent flow (Rossow and Williams, 1979). If such a flow is only weakly forced, then the nonlinear turbulent interactions of eddies, caused by shear instability of the zonal flow, produce a zonal flow resembling solid rotation with most of the eddy kinetic energy in wavenumber 1. The resulting eddy momentum transport is equatorward at most latitudes, opposing poleward advection by the mean meridional circulation. Furthermore, these quasi-barotropic eddies do not transport much heat. However, these two-dimensional model studies do not indicate whether three-dimensional, multicelled meridional circulations will transport momentum to the upper atmosphere or why three-dimensional eddy circulations in slowly rotating atmospheres should behave like two dimensional turbulence.

One other question that has received little attention so far is what process balances the upward transport of momentum from the lower atmosphere. All model studies, discussed above, have employed an *ad hoc* drag or diffusive transport to equilibrate the flow, but no particular mode of motion has been suggested as responsible for downward momentum transport. The angular momentum distribution with latitude near cloud tops (Rossow *et al.*, 1980) precludes downward transport by the direct meridional circulation cell which appears to be present in the clouds (Counselman *et al.*, 1980; Rossow *et al.*, 1980), so downward transport must be provided by some kind of wave motion, possibly the propagating diurnal tides.

c. Three-dimensional model results

The available results from three-dimensional numerical models do not shed much light on the questions raised above. Chalikov *et al.* (1975) used an unrealistic formulation of radiative and turbulent heat fluxes that resulted in a model atmosphere that responds too rapidly to solar heating. This occurs because they equate vertical turbulent heat fluxes between the surface and the first model level to the net *solar* flux at the surface rather than the net *total* radiative flux. The flow which results from this very strong heating is essentially between the subsolar and antisolar longitudes at all altitudes. These results are not relevant to the circulation of the lower atmosphere, where the radiative time scale is much longer than the diurnal time scale; but they may qualitatively describe circulations at much higher altitudes, well above the clouds (cf., Dickinson and Ridley, 1975).

In the three-dimensional model of Young and Pollack (1977), the global mean vertical temperature profile is held fixed, so that the magnitude and dominant mode of the dynamic vertical heat flux cannot be determined from their results. Furthermore, in equilibrium, the horizontal heat flux required to balance differential solar heating is provided almost entirely by the parameterized heat diffusion and not by explicitly calculated motions, so that the realism of the dynamic horizontal heat transport in the model cannot be evaluated. For example, the *direction* of the mean meridional ciculation in the lower atmosphere is different for the two solutions presented, apparently without any effect on the temperature distribution. Although Young and Pollack do obtain a large retrograde zonal flow in the upper model atmosphere, the zonal flow in the bulk of the atmosphere (the lowest 30 km) is prograde in conflict with the observations. In addition, the momentum balance, in equilibrium, is dominated by a parameterized diffusion which does not conserve angular momentum (Rossow *et al.*, 1979). The very low horizontal resolution of the model (the highest wavenumber resolved is 4) and the imposed symmetry about the equator also distort the behavior of the explicitly calculated eddy motions. These properties of the model raise serious questions about the validity of Young and Pollack's conclusions regarding the processes which maintain the strong zonal flow on Venus (Rossow *et al.*, 1979; see also Young and Pollack, 1979).

Hunt (1979) and Williams and Holloway (1982) have both investigated the effects of slowing the planetary rotation rate in three-dimensional, but hemispheric, circulation models of Earth's atmosphere; however, only Williams and Holloway (1982) present results for a rotation rate comparable to Venus, specifically, for a rotation period of 64 days, still four times shorter than for Venus. Both of these studies,

discussed in Sections 4 and 5, provide some qualitative support for the interpretations of the model circulation presented here.

3. Model equations

In standard planetary coordinates, Venus rotates on its axis in the retrograde direction and the predominant zonal wind direction is retrograde, but familiar meteorological coordinates can be used for Venus if positive longitudes are in the direction of planetary rotation and positive latitudes are in the hemisphere containing the positive rotation vector. In these coordinates, the Northern and Southern Hemispheres are reversed and the retrograde zonal wind is a positive zonal wind.

The primitive equations of motion in sigma coordinates ($\sigma = P/P_s$) are divided into the horizontal momentum equations,

$$\frac{\partial}{\partial t}(\mathbf{V}) = -(\zeta + f)\hat{\mathbf{k}} \times \mathbf{V} - \dot{\sigma}\frac{\partial}{\partial \sigma}(\mathbf{V}) - \nabla_H(\tfrac{1}{2}\mathbf{V}\cdot\mathbf{V} + \Phi) - RT\nabla_H(\ln P_s) + \mathbf{F}_m, \quad (1)$$

and the hydrostatic condition

$$\frac{\partial \Phi}{\partial(\ln\sigma)} = -RT. \quad (2)$$

(All of the symbols are defined in the Appendix.) The horizontal momentum equations are changed to the vorticity and divergence equations for a spectral model so that spherical harmonics are eigenfunctions of the homogeneous equations

$$\frac{\partial}{\partial t}(\zeta) = \hat{\mathbf{k}}\cdot\nabla_H \times \mathbf{S}, \quad (3)$$

$$\frac{\partial}{\partial t}(D) = \nabla_H\cdot\mathbf{S}, \quad (4)$$

where $\mathbf{S}$ is the vector on the right in (1).

The thermodynamic equation is

$$\frac{\partial T}{\partial t} = -\nabla_H\cdot(T\mathbf{V}) + T\nabla_H\cdot\mathbf{V} - \dot{\sigma}\frac{\partial T}{\partial \sigma} + F_T + Q_{\text{rad}}C_p^{-1} + \left(\frac{R}{C_p}\right)T[\dot{\sigma}/\sigma + (\mathbf{V} - \tilde{\mathbf{V}})\cdot\nabla_H(\ln P_s) - \nabla_H\cdot\tilde{\mathbf{V}}], \quad (5)$$

where the vertically integrated value of $\mathbf{V}$ is $\tilde{\mathbf{V}} \equiv \int_0^1 \times \mathbf{V}d\sigma$. The term in brackets is just $\omega/P = d(\ln P)/dt$.

The final prognostic variable is $(\ln P_s)$. An equation for the tendency of $(\ln P_s)$ and a diagnostic equation for $\dot{\sigma}$ can be obtained by vertical integration of the mass continuity equation using the boundary condition $\dot{\sigma} = 0$, at $\sigma = 0$ and $\sigma = 1$:

$$\frac{\partial}{\partial t}(\ln P_s) = -\tilde{\mathbf{V}}\cdot\nabla_H(\ln P_s) - \nabla_H\cdot\tilde{\mathbf{V}}, \quad (6)$$

$$\dot{\sigma} = [(\sigma - 1)\tilde{D} + \tilde{D}^*] + [(\sigma - 1)\tilde{\mathbf{V}} + \tilde{\mathbf{V}}^*]\cdot\nabla_H(\ln P_s), \quad (7)$$

where

$$(\tilde{\ })^* \equiv \int_\sigma^1 (\ )d\sigma.$$

The system of equations, (2), (3), (4), (5) and (6), forms a complete set for the prognostic variables, ζ, D, T and $\ln P_s$, with $\dot{\sigma}$ determined diagnostically from (7).

a. Boundary conditions

The only boundary conditions *necessary* for this model are the ones mentioned, namely, $\dot{\sigma} = 0$ at $\sigma = 0$ and $\sigma = 1$. The finite difference formulation of advection in this model requires no further conditions; but vertical diffusion terms, which are not used in this experiment, would require additional boundary conditions on ζ, D and T (see Section 3c). Radiative transfer calculations would also require a top boundary condition and solution of a surface energy balance equation, but the parameterization of radiative heating and cooling employed here requires no boundary conditions (Section 3d).

b. Horizontal diffusion

Since the numerical representation of the advective terms in a spectral model explicitly conserves kinetic energy, the model requires no diffusion terms to maintain the numerical stability of the calculations; however, some dissipation is still required to produce an equilibrium. Such diffusion terms are meant to represent the removal of energy from the resolved scales of motion by interaction with the smaller, unresolved scales of motion (in this case wavenumbers > 15) which are dissipated directly. The horizontal diffusion of momentum becomes diffusion of vorticity in (3) and divergence in (4); *viz.*,

$$\hat{\mathbf{k}}\cdot\nabla_H \times \mathbf{F}_m = \nu[\nabla_H^2\zeta + 2(\zeta/a^2)], \quad (8)$$

$$\nabla_H\cdot\mathbf{F}_m = \nu[\nabla_H^2 D + 2(D/a^2)], \quad (9)$$

where ν is constant. Note that horizontal diffusion of momentum in (8) and (9) vanishes when the atmosphere is either at rest or in solid body rotation. Temperature (i.e., heat) diffusion in (5) is given by

$$F_T = (\nu \text{Pr}^{-1})\nabla_H^2 T, \quad (10)$$

where the Prandtl number $\text{Pr} = 1$.

c. Vertical diffusion and the surface boundary layer

Since the objectives of this study concern vertical fluxes of heat and momentum by explicitly resolved motions, both of which may be extremely weak (see

discussion in Section 5), parameterized vertical diffusion of heat and momentum are completely neglected in this model except for the interactions between the lowest atmospheric level and the planetary surface. In this way the vertical transports by the explicit dynamical modes can be studied in isolation.

The lowest model level is assumed to be the top of the planetary boundary layer where surface effects go to zero. The momentum and heat transports caused by boundary layer turbulence are formulated as bulk drag forces

$$\{\mathbf{F}_m, F_{Ts}\} = (g/P_s)\frac{\partial}{\partial\sigma}\{\tau, \eta\}, \tag{11}$$

where the stresses τ and η, are zero at the top of the boundary layer and equal to

$$\tau_s = \rho_9 C_D|\mathbf{V}_9|\mathbf{V}_9, \tag{12}$$

$$\eta_s = (P/P_0)(R/C_p)\rho_9 C_D|\mathbf{V}_9|(\Theta_s - \Theta_9), \tag{13}$$

at the surface. Here, P_0 is the reference pressure used to define the potential temperature Θ, and the velocity vector has horizontal components only. The subscripts s and 9 refer to the surface and model level nine (lowest), respectively. The expression (12) holds when the surface wind velocity is zero and surface topography effects are neglected; however, use of $\mathbf{V}_9$ in (12) rather than some estimated surface wind probably overestimates drag effects on the first model level. Since there is no surface energy balance calculation in the model (see Section 3d), Θ_s is undetermined. For convenience, the boundary layer is assumed to be well-mixed, i.e., adiabatic, so that $\Theta_s = \Theta_9$ in (13). This approximation is no more accurate than calculating Θ_s by extrapolation once equilibrium temperatures are established.

d. Radiative heating and cooling

Calculation of the radiative flux divergence in the model atmosphere is replaced by a Newtonian relaxation of the temperature toward a specified temperature distribution which represents radiative equilibrium in the absence of any dynamics:

$$Q_{\text{rad}}/C_p = (T_{\text{eq}} - T)\tau_{\text{rad}}^{-1}, \tag{14}$$

where τ_{rad} represents a radiative relaxation time. Detailed radiative heating calculations do not seem appropriate, given the uncertainties in composition and distribution of absorbers in Venus' atmosphere (cf. Tomasko *et al.*, 1980b). Furthermore, the large amount of computer time required to reach thermal equilibrium can be considerably decreased by avoiding radiative transfer calculations in the model. Although the simple form (14) cannot represent all of the complex relationships which determine the radiative flux divergence, qualitatively good results are obtained near equilibrium by using estimates of T_{eq} and τ_{rad} from more detailed calculations (Pollack and Young, 1975). The following approximations are made.

1) T_{eq} and τ_{rad} are functions of σ. Since P_s is nearly constant, this makes T_{eq} and τ_{rad} functions of pressure. This approximation does not completely represent the dependence of radiative heating/cooling on atmospheric density.

2) The values of T_{eq} used represent radiative equilibrium without dynamic motions; consequently, the equilibrium temperature attained by the model will differ from T_{eq} in regions of convection or strong dynamic heat transport. This lessens the validity of the particular values of T_{eq} used, especially in the model lower atmosphere.

3) The solar zenith angle effect on T_{eq} is represented by the simplest function of latitude, $T_{\text{eq}} = (4/\pi)T^* \cos\theta$, and neglects diurnal heating variations. T^* is the global mean radiative equilibrium temperature. This assumption exaggerates the strength of solar differential heating somewhat since T_{eq} at the poles is zero; however, scaling analysis of Hadley circulations with statically unstable radiative states (Stone, 1974) shows that the equilibrium equator-to-pole temperature gradient and the strength of the Hadley circulation are only weakly dependent on the magnitude of the radiative equator-to-pole temperature gradient.

e. Other model physics

Whenever the temperature lapse rate exceeds the adiabatic lapse rate, the atmosphere becomes hydrodynamically unstable to small-scale convective motions which rapidly transport heat vertically. This heat transport is represented in the model by a dry convective adjustment (Manabe *et al.*, 1965) which maintains the temperature lapse rate slightly (1%) subadiabatic. Momentum transport by these turbulent motions is neglected. Although water vapor and clouds are present in Venus' atmosphere, the observed cloud mass density is too small to cause any important latent heat effects (Rossow, 1978). Cloud radiative effects are, however, incorporated in the estimates of T_{eq} used in the model (see Section 4).

f. Parameter values

Table 1 shows the physical and model parameters used for this calculation. The values of a, g and Ω are from Allen (1973). The value of R is for a mean molecular weight of 41.4 and the value of C_p is for an ideal carbon dioxide gas at Venus surface conditions (cf. Staley, 1970). Since the variation of C_p with temperature is neglected here, these values are somewhat arbitrary; but the precise values of R and C_p are not crucial. The only crucial thermodynamic rela-

TABLE 1. Parameters used in the model.

Physical parameters

Planetary radius a = 6050 km
Surface gravity g = 8.6 m s^{-2}
Planetary rotation frequency $\Omega = 2.98 \times 10^{-7}$ s^{-1}
Mean surface pressure $\bar{P}_s = 9 \times 10^6$ Pa
Gas constant R = 201 J K^{-1} kg^{-1}
Specific heat C_p = 5.6 R
Horizontal diffusivity $\nu = 2 \times 10^5$ m^2 s^{-1}
Surface drag coefficient C_D = 0.002

Numerical parameters

Truncation wavenumber J = 15
Number of latitude circles IY = 40
Number of longitudinal meridians IX = 64
Number of vertical levels k_0 = 9
Time step Δt = 2700 s
Time filter constant α = 0.03

Level No. (k)	$\sigma_k P$ (10^3 Pa)	$\sigma_{k-1/2} P$ (10^3 Pa)	T^* (K)	τ_{rad} (days)
1	11.2	0	250	43
2	41.5	22.3	275	220
3	113	60.6	320	666
4	306	165	390	1447
5	705	448	410	1562 (2894)*
6	1220	961	440	1620 (4340)
7	2160	1920	520	1736 (7812)
8	4730	3310	700	1852 (12730)
9	7580	6160	950	1852 (18520)
—	—	9000	—	—

* Pollack and Young (1975) values are shown in parentheses when different values are used in the model.

tionship is that the model adiabatic lapse rate, Γ = 7.6 K km^{-1} is smaller than the radiative equilibrium temperature lapse rate in the lower four model levels and larger than it is in the upper model levels.

The value of C_D is unknown for Venus, but may be somewhat smaller than that used here which is characteristic of the surface stress on Earth at ~100 m altitude (Miyakoda and Sirutis, 1977). At the height of the lowest model level (2.6 km) with a mean zonal wind speed of ~0.1 m s^{-1}, this value of C_D gives a drag time constant, $\tau_{drag} \sim$ 200 days. The value of ν for Venus is also unknown; the value used here is the same value used in this model to simulate Earth's circulation (Gordon and Stern, 1982) and is just large enough to restrain the increase in kinetic energy in the smallest scales of motion without affecting the larger scales (the diffusion time constant τ_ν is ~100 days for wavenumber 15 and ~20 000 days for wavenumber 1). Although this choice results in a flat kinetic energy spectrum in low model latitudes, suggesting the need for stronger dissipation, this behavior is similar to the low-latitude behavior of this numerical model with Earth parameters. Since the flat spectrum in the simulated Earth tropics seemed to be independent of the model resolution used (W. F. Stern, 1977, private communication), there is no compelling reason to increase the importance of the parameterized diffusive transports relative to the explicit motion transports.

The values of T^* and τ_{rad} are from the one-dimensional radiative equilibrium calculation of Pollack and Young (1975), which includes the effects of a sulfuric acid cloud extending down to the 10-bar level and a constant water vapor mixing ratio of 0.3% below the clouds. Pioneer Venus and Venera probe measurements show that the clouds only extend to the 2-bar level (Knollenberg *et al.*, 1980) and that the water vapor mixing ratio may be lower than 0.3% (Marov, 1978). Nevertheless, the qualitative variation of Pollack and Young's values are all that are crucial to this experiment. In particular, most of the solar energy is deposited in the clouds, but a large infrared opacity in the lower atmosphere produces a strongly superadiabatic temperature lapse rate in radiative equilibrium. These properties enhance the role of small-scale convection in the model lower and upper atmosphere while suppressing it at intermediate levels (see Fig. 2).

The major approximation made in this model is the choice of the values of τ_{rad} in the lower atmosphere, which are smaller than the values estimated by Pollack and Young (1975). This approximation is necessary to reach thermal equilibrium in a reasonable amount of computer time. The values shown in Table 1 further exaggerate the importance of convection by increasing heating rates in the lower atmosphere where the mean meridional circulation is insensitive to the heating rate (Stone, 1974); but the crucial qualitative relationships between thermal and dynamic time constants, which make the Venus circulation unique, namely, $\tau_{rad} \gg \tau_{dyn}, \tau_\nu, \tau_{drag}, \tau_{day}$ (Stone, 1975), are maintained ($\tau_\nu \ll \tau_{rad}$ for wavenumbers > 7).

g. *Numerical model*

Eqs. (2), (3), (4), (5) and (6) are solved with a spectral numerical model which is identical, except for

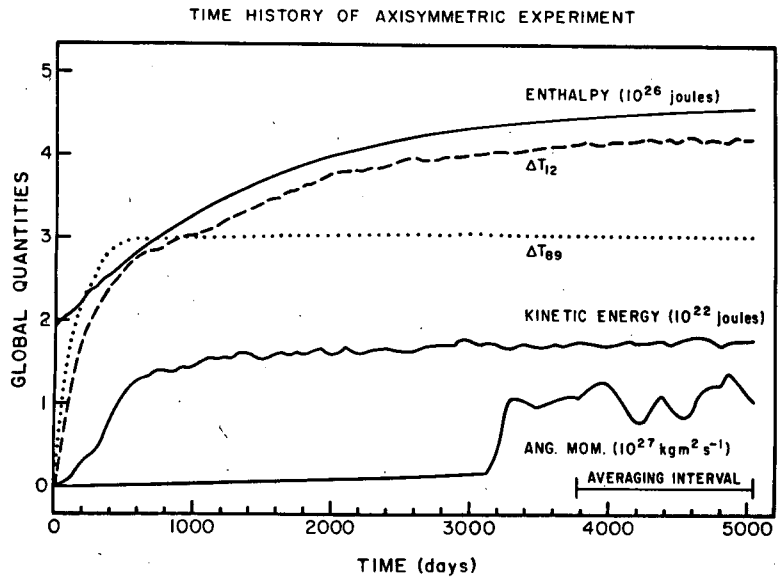

FIG. 1. Time evolution of global mean quantities: total enthalpy, total kinetic energy, total angular momentum, and the temperature contrasts between two pairs of constant pressure surfaces, ΔT_{12} between 11.5×10^3 and 41.5×10^3 Pa and ΔT_{89} between 4730×10^3 and 7580×10^3 Pa. The curves have been smoothed with a 120-day running average. Time averaged quantities discussed in the paper are calculated for the interval indicated.

the changes discussed above, to one model of the Earth's atmosphere used by the Experimental Prediction Group at GFDL (Gordon and Stern, 1982). The calculations were performed on the GFDL ASC computer. In the model, the variables are represented on each of nine vertical levels by a series of surface spherical harmonics Y_L^M, truncated by $-J \leq M \leq J$ and $|M| \leq L \leq |M| + J^*$, where $J = 15$ and $J^* = J$ or $J + 1$ depending on the particular variable. The nonlinear terms are calculated by transforming all the variables to a latitude–longtitude grid large enough to prevent aliasing, forming the nonlinear products, and transforming them back to a spectral representation. Prognostic variables are defined on the "full" model levels while $\dot{\sigma}$ is defined on "half" levels. The time differencing scheme is a modified version of the semi-implicit leapfrog scheme with a filter proposed by Robert (Bourke *et al.*, 1977). For a more complete description of the model, see Gordon and Stern (1982).

The performance of this model has been thoroughly tested and compared to gridpoint models and higher resolution spectral models (Gordon and Stern, 1982). These tests demonstrate the ability of this model to simulate all of the fundamental instabilities of the large-scale circulation. Although the vertical resolution has been reduced for the calculations presented here, especially in the upper atmosphere, the lower atmosphere (two scale heights) is resolved into five layers which is still sufficient to simulate the primary modes of instability (cf. Held, 1978).

4. Model mean circulation

Initial conditions for this experiment are an isothermal (250 K) atmosphere at rest. The model circulation approaches equilibrium before the end of a 5060-day integration, as Fig. 1 shows. Description of the equilibrium circulation focuses on the time-averaged properties determined from the last 1280 days of the integration. Fig. 1 illustrates the effects of the explicitly defined time constants on the model circulation: the evolution of the total enthalpy reflects the radiative relaxation time (~1800 days) of the lowest, most massive portion of the atmosphere, and the growth and oscillation of the total angular momentum reflect the surface drag time (~200 days).[4] The evolution of the temperature gradient between the upper two levels also reflects the long time constant of the total enthalpy as a consequence of an increasing dynamic heat flux from the lower to the upper atmosphere, a situation analogous to the moderating influence of Earth's oceans on the atmosphere (see discussion in Section 4c).

The total kinetic energy evolves on a time scale (~500 days) which is shorter than the forcing time scale of radiation but longer than the dissipation time scales of surface drag or diffusion of the smaller scale

[4] The change in the growth rate near day 3200 was caused by correction of a code error which produced, in the first part of the integration, a surface drag coefficient several orders of magnitude smaller than intended; the evolution subsequently reflects the 200-day time constant.

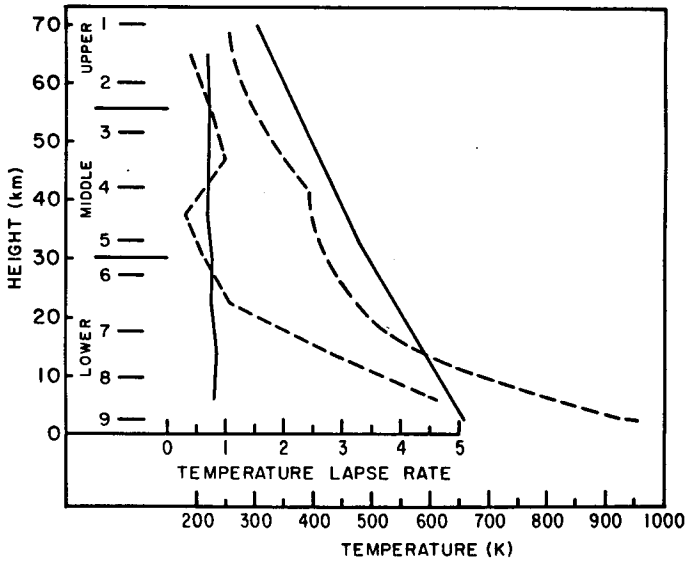

FIG. 2. Horizontally averaged vertical temperature structure (right) and lapse rate (left) in model equilibrium (solid) and in radiative equilibrium (dashed). The lapse rate is expressed as a ratio of the actual and adiabatic lapse rates. Three atmospheric regions are defined and the approximate altitudes of the model sigma surfaces shown.

(wavenumber > 6) eddies. A comparison of the decrease in kinetic energy caused by a three-order-of-magnitude increase in the surface drag coefficient (Fig. 1) with that caused by a factor of 10 increase in the horizontal diffusivity (not shown) shows that horizontal diffusion dominates energy dissipation in the model, but *total* kinetic energy is less sensitive to the diffusivity than kinetic energy at high (>6) wavenumbers. This behavior, together with the intermediate evolution time scale shown in Fig. 1, suggests that the dissipation rate of total kinetic energy depends on the nonlinear cascade rate of energy from larger to smaller scales. The weak dependence of this cascade rate on either the radiative time constant or the diffusivity argues that the dynamic time scale in Fig. 1 is only indirectly related to the specified model time scales.

In Fig. 1 the vertical temperature gradient in the lower atmosphere equilibrates on about the same time scale as the overturning time of the mean meridional circulation (see Section 4b), which is shown to be consistent with Stone's (1974) hypothesis that this should happen in a slowly rotating, massive atmosphere when the radiative equilibrium temperature lapse rate is superadiabatic (see Section 5a). This behavior also implies that the horizontal temperature gradient equilibrates on the same time scale, since the mean meridional circulation provides all of the horizontal heat flux in the model lower atmosphere. In effect, the efficient dynamic control of the thermal contrasts maintains a roughly constant differential radiative heating rate regardless of the *mean* temperature of the lower atmosphere; consequently, the relaxation time of the thermally driven circulation is independent of the radiative relaxation time as long as $\tau_{rad} \gg \tau_{dyn}$. Furthermore, since the strength of the thermal circulation is insensitive to the strength of the solar heating rate [Stone (1974) shows that the mean meridional velocity in equilibrium is proportional to the one-third power of the radiative equilibrium vertical temperature gradient], the behavior shown in Fig. 1 justifies, *a posteriori*, the choice of τ_{rad} used in the model.

a. Mean thermal structure

The time-averaged thermal structure is illustrated in Figs. 2, 3 and 4. Despite exaggerated radiative forcing of horizontal and vertical temperature contrasts in the model, the atmosphere is statically stable and nearly barotropic. In Fig. 2, the global mean vertical temperature profile exhibits a monotonic increase of static stability[5] from ~20% in the lower atmosphere to ~35% in the upper atmosphere. The lower atmosphere[6] is a region strongly heated and destabilized by radiation, while the middle and upper regions are cooled and stabilized, except for a region between 42 and 52 km. The differential radiative heating/cooling

[5] The percent static stability values in the text are expressed as one minus the values shown in Fig. 2.

[6] The regions of the atmosphere called lower, middle and upper are defined in Fig. 2 and will be used throughout this paper. The discussion in this section shows that these regions are marked by differences in their structure and their heat/momentum budgets.

with altitude is balanced by a dynamic vertical heat transport from lower to upper atmosphere (see Section 4c). The horizontal temperature distribution, in Fig. 3, exhibits a large-scale decrease of temperature from equator to pole in the lower and upper atmosphere; but at all levels the temperature contrasts are

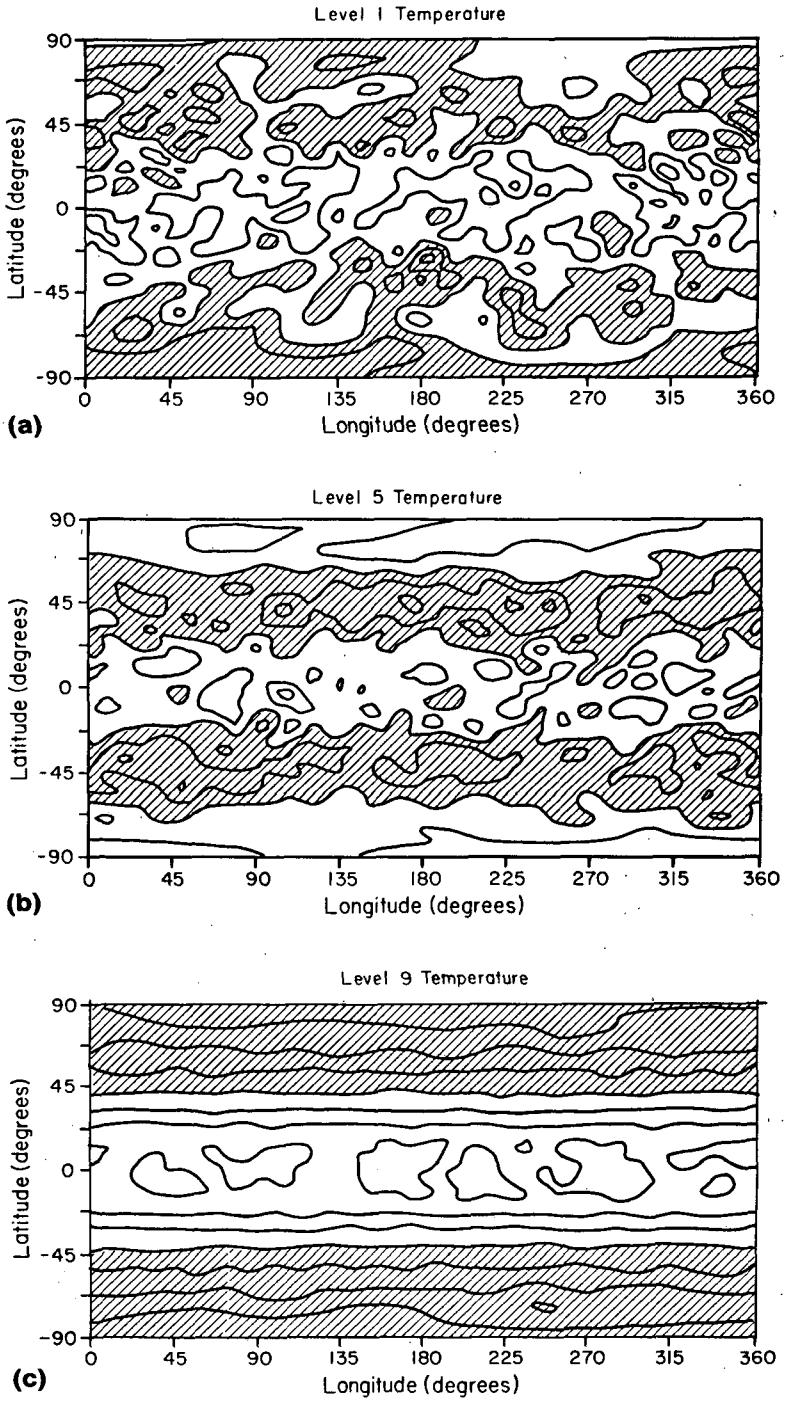

FIG. 3. Time-averaged horizontal distribution of temperature for three model sigma surfaces. Shading indicates temperatures below some reference value T_0. The reference temperatures and contour intervals ΔT are (a) for level 1 T_0 = 299 K, ΔT = 2 K; (b) for level 5, T_0 = 476.6 K, ΔT = 0.8 K; and (c) for level 9, T_0 = 658 K, ΔT = 1 K. These temperature contrasts are slightly larger than those on constant pressure surfaces.

only ~1% of the radiative equilibrium equator-to-pole contrast. Relative to the mean temperature, these horizontal gradients are about an order of magnitude smaller than those on Earth, implying much more efficient dynamic horizontal heat transport.

The mean thermal structure, together with the distribution of small-scale convection (see Fig. 6d), is evidence that a simple balance between radiation and convection is not responsible for the static stability exhibited by the model atmosphere. Although radiation destabilizes lower altitudes (Fig. 2) and lower latitudes (Fig. 6a), while stabilizing higher altitudes and latitudes, there is a much more complicated variation of static stability with altitude and latitude (Fig. 4). In the time mean, the occurrence of convection is only partially correlated with the regions of low static stability shown in Fig. 4. For example, convection occurs near 45° latitude between model levels 5 and 6 (Fig. 6d), but not at high latitudes between levels 8 and 9 where the static stability is lower (Fig. 4). Small-scale convection actually only occurs very sporadically in the model; only the convection in the region between ±10° latitude in the lower atmosphere can be said to be continuous. Even there the zonal mean static stability is ~15%, which requires vertical heat transport by processes other than convection (see Section 4c). The static stability distribution for the lower atmosphere is, however, strongly correlated with the mean meridional circulation pattern (Fig. 5b) with low stability associated with upward motions. This relationship, together with the relative contribution of convection to the heat budget (see Section 4c), suggests control of the static stability by the mean meridional circulation.

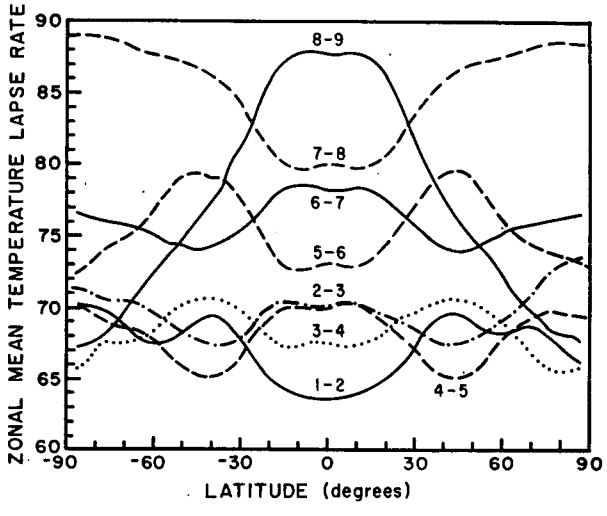

FIG. 4. Zonal mean temperature lapse rate between constant pressure surfaces as a function of latitude. The lapse rates are expressed as a percentage of the adiabatic value in pressure coordinates. Pressures for model levels (numbers on curves) are given in Table 1.

b. Mean circulation

The time and zonally averaged meridional, vertical and zonal velocities in equilibrium are presented in Fig. 5. The meridional circulation defines three different regions. In the lower atmosphere, the mean meridional circulation takes the form of three cells in each hemisphere, a direct cell near the surface, an indirect cell above, and another direct cell above that. These cells extend from equator to pole with the downdraft and updraft regions occupying about the same surface area; however, the contours in the updraft region near the surface indicate a rather broad maximum, while the contours in the downdraft region show a narrow maximum near the poles. The hemispheric mean meridional wind speed is ~2 m s^{-1}, implying an overturning time scale of ~5×10^6 s. The meridional circulation in the upper atmosphere takes the form of a single, direct, equator-to-pole cell with slightly smaller wind speeds than in the lower atmosphere. These two meridional circulations are the strongest and coincide with the two maxima in the vertical distribution of radiative heating (Fig. 6a).

The circulation in the middle atmosphere is much weaker and more complex than in either the upper or lower atmosphere and coincides with a minimum in the radiative forcing (Fig. 6a) caused by the deep cloud included in Pollack and Young's (1975) calculations. This meridional circulation joins the equatorward flow of the direct cell in the upper atmosphere to the poleward flow of the upper direct cell in the lower atmosphere; but instead of a single indirect cell, the circulation is more complicated in altitude and latitude. The predominant pattern is two cells in each hemisphere, with a direct cell at higher latitudes and an indirect cell at lower latitudes. However, the large differences between the hemispheres in Figs. 5a and 5b testify to a large time variation of the circulation in the middle atmosphere, making it difficult to characterize the mean flow very precisely.

The mean meridional circulation cells shown in Fig. 5a exhibit a variety of depths, indicating that something more than atmospheric density controls the depth of such circulations. In Earth's tropical atmosphere, the Hadley circulation extends over a little more than one scale height up to a sharp change in the static stability at the tropopause. A similar, but smaller, change in static stability occurs at 33 km in the model (the global mean static stability below 33 km is ~21% and ~32% above), yet three circulation cells form over the lowest two scale heights of the lower atmosphere. In contrast, the circulation cell in the upper atmosphere extends over a little more than one scale height, while those in the middle atmosphere extend over three scale heights even though there is little difference in the static stability between the upper and lower atmospheres. Part of these dif-

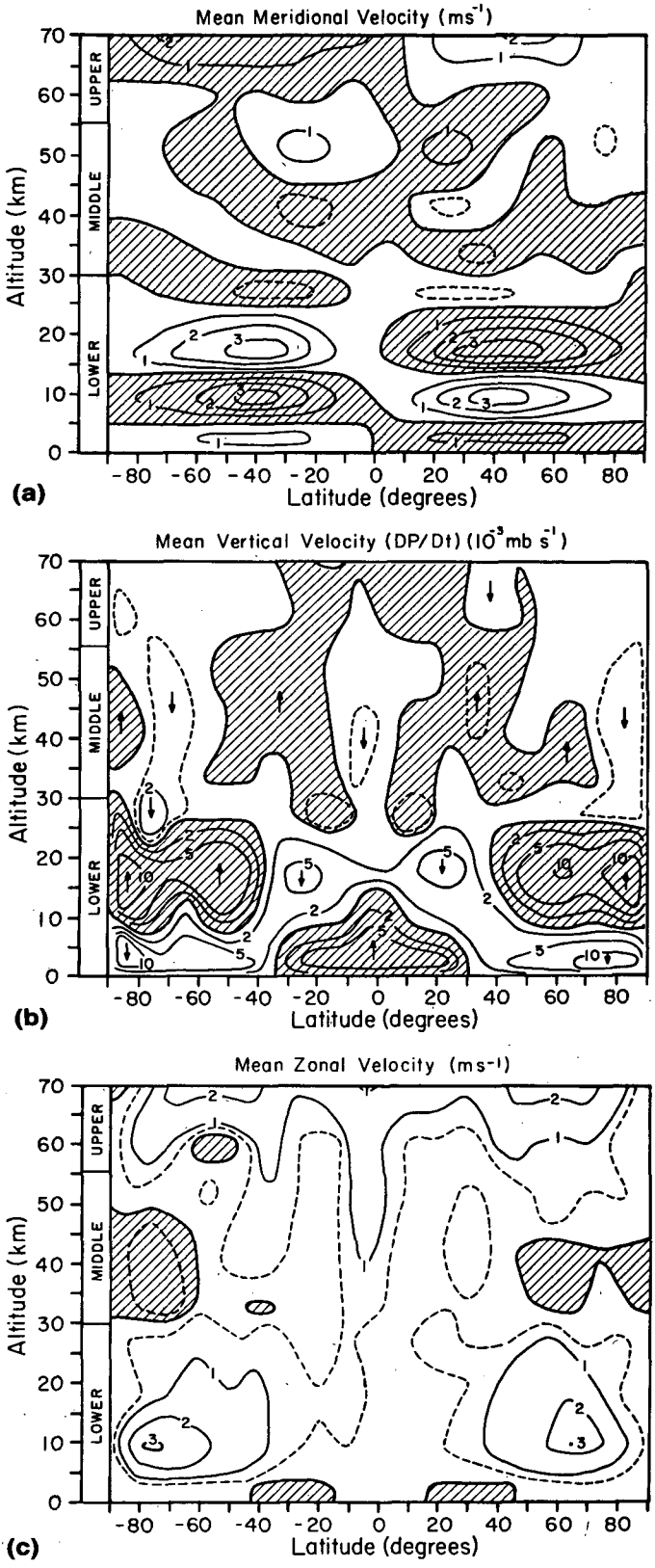

FIG. 5. Zonal mean wind components as a function of altitude and latitude for three altitude regimes: (a) meridional wind (positive is northward, (b) vertical wind (positive is downward), and (c) zonal wind (positive is in direction of planetary rotation). Dashed contour represents half the value of the smallest solid contour value.

ferences may be caused by the coarse vertical resolution, but the correlation of these cells with the vertical distribution of heating and cooling, discussed in Section 4c, suggests that it is the heating/cooling distribution which controls the pattern of the meridional circulation. The model results of Kalnay de Rivas (1973, 1975) also support such a conclusion.

Fig. 5c shows nothing like the strong zonal winds observed in Venus' upper atmosphere, but the zonal flow is generally positive[7] everywhere except for two regions near the surface at lower latitudes and at higher latitudes in the middle atmosphere. The negative zonal flow at the surface is necessary *in equilibrium* to insure zero net surface wind torque on the planet on average (see Section 4d). The global mean angular momentum of the model atmosphere is, however, positive at all altitudes (see Fig. 13), with a strong concentration of angular momentum in the poleward branch of the surface Hadley circulation near 10 km altitude. This superrotation of the whole atmosphere with respect to the planet is a fundamental difference between this dynamic regime and an Earth-like (rapidly-rotating) dynamic regime (see Section 4d).

The mean zonal flow, shown in Fig. 5c, has five jets, four at mid-to-high latitudes associated with the poleward branches of the two strongest direct meridional circulation cells in the upper and lower atmosphere, and one equatorial jet associated with the low-latitude indirect circulation in the middle atmosphere. The midlatitude jets in the upper atmosphere are actually much stronger (5–15 m s^{-1}) and narrower than indicated, but their location ranges from 40 to 80° latitude and is more variable than the jets in the lower atmosphere. The time variation in the magnitude and location of all of the mid-to-high latitude jets is quasi-periodic and only occasionally coordinated in the two hemispheres at a given altitude. These large variations indicate the predominance of eddy motions in the circulation; total eddy kinetic energy in the model is 10 times greater than the zonal kinetic energy. Large-scale and slow eddy motions are also responsible for the small asymmetries in the time mean winds presented in Fig. 5.

c. *Heat budget*

The basic zonally averaged components of the heat budget[8] are shown in Fig. 6 as a function of altitude and latitude. The heating/cooling rate caused by the parameterized horizontal heat diffusion is an order of magnitude smaller than any of the components shown. The balance, integrated over the whole atmosphere, is between differential radiative heating and differential cooling by the dynamics. The mean meridional circulation provides a little more than half of the dynamic cooling, but this nearly equal division of differential cooling is actually the result of net horizontal heat transorts entirely by the mean meridional circulation and net vertical heat transports dominated by eddies.

The *net* radiation in Fig. 6a generally heats lower latitudes and cools higher latitudes, but the lower latitude heating has a relative minimum in the middle atmosphere. The meridional circulation in Fig. 6b generally cools lower latitudes and heats higher latitudes to balance the horizontal variation of radiative heating/cooling, except for a core of heating extending from 10–60 km produced by the indirect meridional circulations between 10 and 20 km and at low latitudes in the middle atmosphere. In general, the eddies cool the lower atmosphere below ~15 km and heat the upper atmosphere near 60 km to balance the vertical variation of radiative heating/cooling.[9] However, the eddy heating/cooling is confined to three latitude zones in the lower and middle atmosphere, which coincide with regions of convective activity (Fig. 6d). The strong eddy heating of the upper atmosphere is concentrated near 60 km by strong radiative damping of the propagating waves (see Section 4e) near 70 km. This heating drives widespread, though sporadic, convection at most latitudes (Fig. 6d), despite a stable radiative equilibrium state.

At any particular location, the vertical heat flux by the mean meridional circulation is much larger than that provided by eddies or convection; however, the *net* vertical flux of heat by the meridional circulation is weak as a consequence of the near-cancellation of the vertical fluxes in the updraft and downdraft portions of a single cell, as well as some cancellation between the fluxes of direct and indirect circulations. In the lower atmosphere the net vertical flux by the meridional circulation is still comparable to that by the eddies and convection, but the transport of heat from there into the middle and upper atmosphere is entirely by eddies and convection. Even though the vertical heat flux averaged over the lower atmosphere is produced approximately equally by the mean meridional circulation, convection and eddies, most of the eddy and convective heat flux occurs near the equator (Figs. 6c and 6d). Consequently, the mean meridional circulation controls the static stability as suggested by the correlation of the patterns in Fig. 4 with the mean updraft/downdraft locations.

Horizontal heat transports are dominated by those of the meridional circulation both locally and globally. Even when integrated over the entire atmo-

[7] Zonal flow in the direction of planetary rotation will be referred to here as positive or westerly zonal flow so that discussion of angular momentum balance has the same sense as on Earth.

[8] As Fig. 1 illustrates, the model atmosphere is still heating slowly (~0.04 K day^{-1}).

[9] The large cooling rates at the poles in Fig. 6c are artifacts of the diagnostics calculations, which are not present in the actual model calculations.

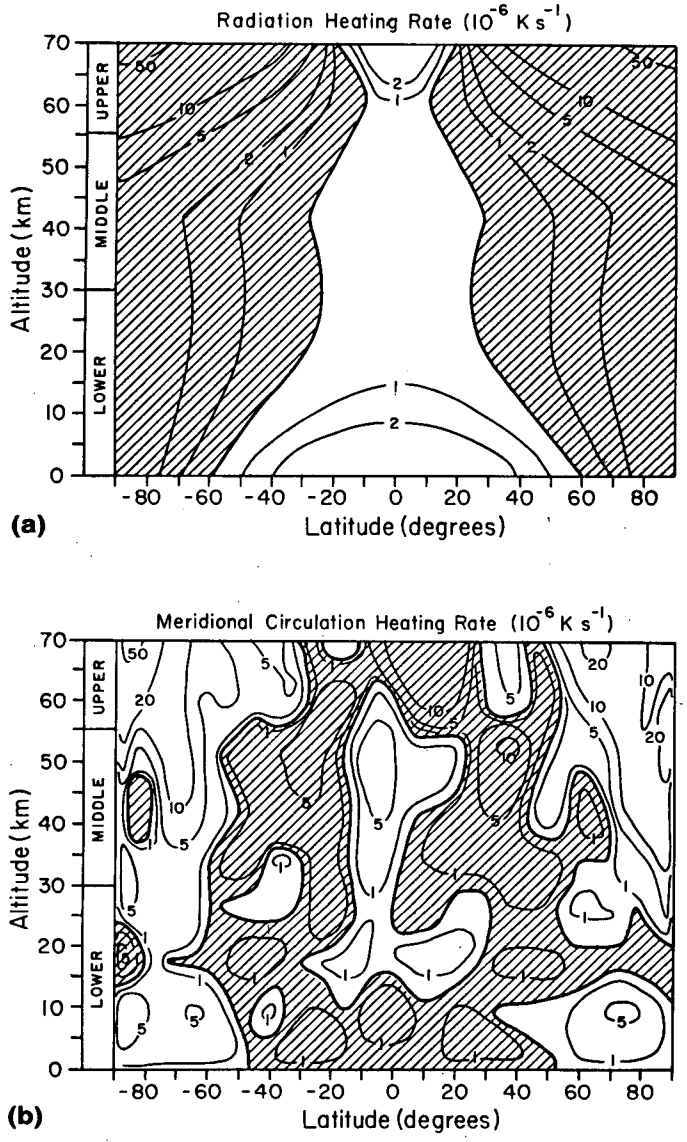

FIG. 6. Zonal mean heating/cooling rates, as function of altitude and latitude, caused by (a) radiation, (b) meridional circulation, (c) eddies and (d) convection. Heavy lines are the zero contour and shading indicates regions of cooling.

sphere, the horizontal transport of heat by eddies is only 2% of that by the meridional circulation. Most of this heat transport is provided by the eddies in lower latitudes. Consequently, the horizontal temperature gradients in the lower atmosphere, established in equilibrium, are controlled entirely by the balance between differential radiative heating and heat transport by the mean meridional circulation, as expected from laboratory fluid dynamics experiments. Despite the multiple circulation cells in the vertical, the vertically integrated heat transport of the mean meridional circulation has the same latitudinal distribution as a single Hadley cell.

The vertical structure of the mean meridional circulation does not appear to coincide with variations of atmospheric density or static stability; the cells in Fig. 5a vary from one-half to two scale heights in depth. Instead, the vertical structure of the mean meridional circulation correlates only with vertical variations in net heating/cooling near the equator, influenced strongly by the convective and eddy heating/cooling distributions, as shown by comparing Fig. 5a with Fig. 7. The sum of the contributions of radiation, convection and eddies to heating/cooling near the equator produces a vertical pattern which mirrors that of the meridional heating/cooling. The

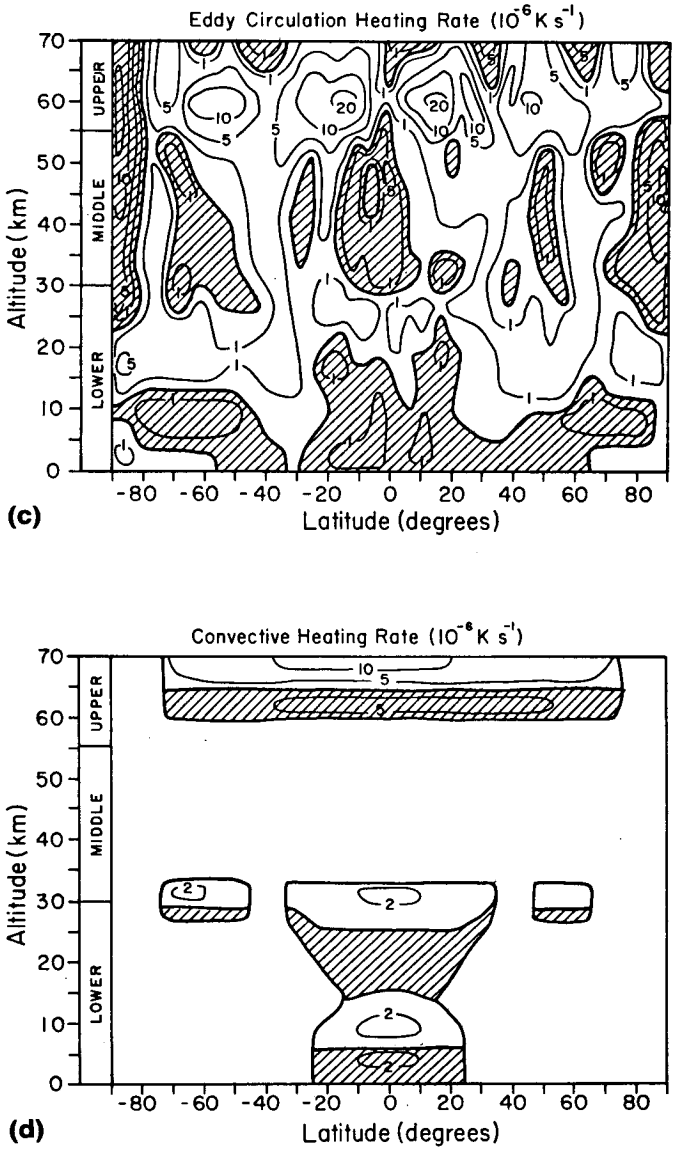

FIG. 6. (*Continued*)

strong meridional circulation in the upper atmosphere is primarily driven by eddy heating concentrated near 60 km but redistributed upward by stimulated convection. This coupling to the lower atmosphere explains the evolution of the upper atmospheric vertical temperature lapse rate in Fig. 1. The indirect meridional circulation at lower latitudes in the middle atmosphere is associated with net cooling at the equator by the eddies. This is part of a pattern of eddy heating/cooling associated with the three zones of convection (Figs. 6c and 6d), which shifts the net (radiative plus eddy) heating between 27 and 60 km away from the equator to midlatitudes. This shift explains the midlatitude temperature maximum (Fig. 3b) and the mean meridional circulation (Fig. 5b) in the middle atmosphere. In the lower atmosphere the eddies slightly weaken the equator-to-pole contrast driving the meridional circulation, while the convection shifts some of the heating to higher levels (Figs. 6c, 6d and 7), producing the three maxima exhibited by the meridional circulation cooling at low latitudes and the triple-cell structure of the meridional circulation (Fig. 6b).

d. Momentum budget

The angular momentum of the model mean zonal flow (Fig. 5c) is positive at all altitudes (Fig. 13); i.e., the model atmosphere superrotates as does that of Venus, although the total angular momentum of the

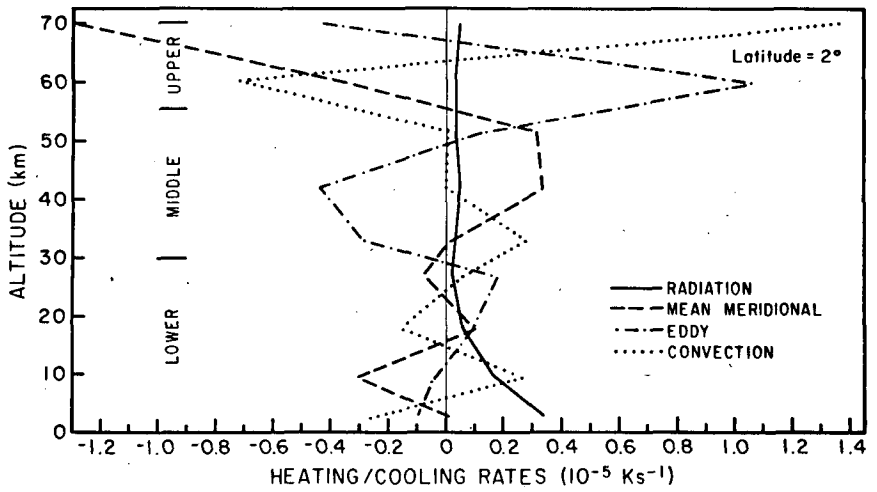

FIG. 7. Zonal mean heating/cooling rates at 2° latitude as function of altitude.

model atmosphere is an order of magnitude smaller. The model momentum budget only involves transports by the mean meridional circulation and explicitly resolved eddies, with surface drag important in the lowest model level; parameterized horizontal eddy diffusive transports are an order of magnitude smaller than the resolved transports and parameterized convective transport is zero by assumption. Averaged over the last 1280 days and integrated over the whole atmosphere, the meridional circulation produces a net upward and poleward angular momentum flux, while the eddies produce a net downward and equatorward flux, with the net surface torque equal to zero. This angular momentum budget is essentially that postulated by Gierasch (1975) to explain the large zonal wind speeds in the cloud top region on Venus; but, as discussed below and in Section 4, the eddies which produce the equatorward momentum transport are different from the eddies responsible for the downward momentum flux.

Positive angular momentum at all altitudes precludes production of the zonal flow in the model solely by momentum conserving exchanges between different atmospheric levels, but requires some transfer of angular momentum from the solid planet to the atmosphere. If the surface interaction with the wind is formulated as a drag law, as in this model, then negative zonal surface winds are required somewhere to transfer angular momentum from the planet to the atmosphere. Once a positive zonal flow has built up, equilibrium is established by the drag exerted on positive zonal winds. Thus, near surface zonal winds in both directions are required in an atmosphere with positive total angular momentum and zero net surface torque in equilibrium (cf. Fig. 5c).

Fig. 8 shows the horizontal transport of angular momentum by the meridional circulation and the eddies. The direction of transport by the meridional circulation (Fig. 8a) is strongly correlated with the meridional wind direction (Fig. 5a) as expected; but the net transport is poleward when vertically integrated over the upper and lower atmosphere and nearly zero in the middle atmosphere, producing zonal jets at higher latitudes near 10 and 70 km. The eddy momentum transport throughout the atmosphere is generally equatorward, except near the equator, but the eddy transports in lower latitudes exhibit alternating directions of transport which weaken their net area-averaged effect there. A similar pattern of eddy transports is also exhibited in the upper and middle atmosphere, but the large time variations and mixture of two types of eddy motions (see Section 4e) make the pattern more complex.

As Gierasch (1975) pointed out, the consequence of a horizontal angular momentum transport by eddies opposing that by the meridional circulation is an equatorward shift of the zonal flow distribution with latitude compared to that produced by conservative poleward advection. Thus, the downdraft branch of the meridional circulation at higher latitudes carries down less angular momentum that brought up by the updraft branch causing the meridional circulation to transport angular momentum upward, on average. Fig. 9a shows the vertical flux of angular momentum by the multicellular meridional circulation. The horizontal offset between the locations of the peak vertical fluxes in the direct and indirect circulations in the lower atmosphere allows for net upward momentum transport by the multicellular circulation. Thus, despite the complex structure, the average flux is stronger at the equator than at higher latitudes, and the flux, averaged over the whole atmosphere, is upward.

Fig. 9b shows that the downward eddy momentum flux is provided entirely by the eddies near the equator, which are predominantly the eddies stimulated

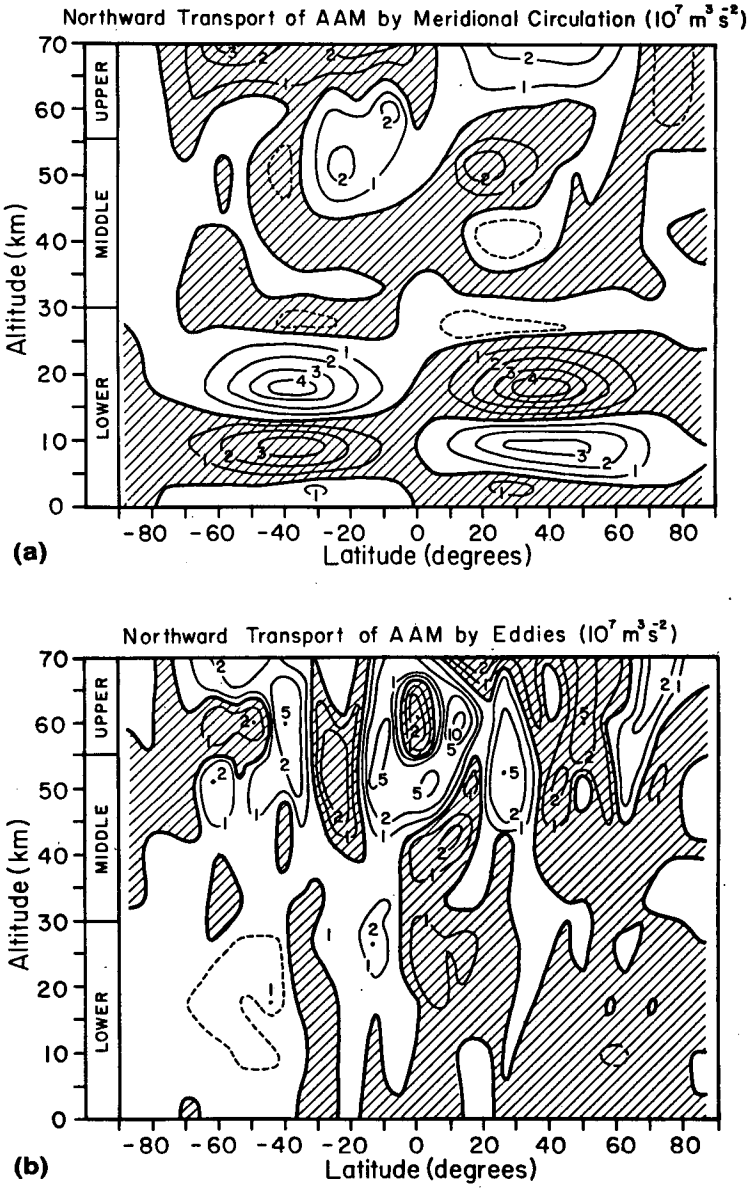

FIG. 8. Zonal mean northward transport of absolute angular momentum, as a function of altitude and latitude, caused by the meridional circulation (a) and eddies (b). Heavy line is the zero contour and shading indicates southward transport. The dashed contours are for 0.5×10^7 m^3 s^{-2}.

by convection (see Section 4e), while the eddies associated with the zonal jets at higher latitudes are responsible for an upward flux of angular momentum. This identification of a particular direction of transport with the two different types of eddy is not evident in Fig. 9b; however, the different character of the eddy statistics in the two latitude zones strongly suggests such an interpretation (Section 4e).

Despite the removal of a major forcing of eddy motions, diurnal solar heating, the model heat and momentum budgets involve very complex interactions between the mean flow and at least two types of explicitly resolved eddies (see Section 4e). Parameterized small-scale convection plays no direct role in the momentum budget, by assumption, but still plays an important indirect role. As will be discussed in Section 4e, the convection's penetration into the statically stable middle atmosphere produces vertically propagating gravity waves which are primarily responsible for the downward eddy momentum transport in the model. While this process is plausible, the amplitude of the heat and momentum fluxes pro-

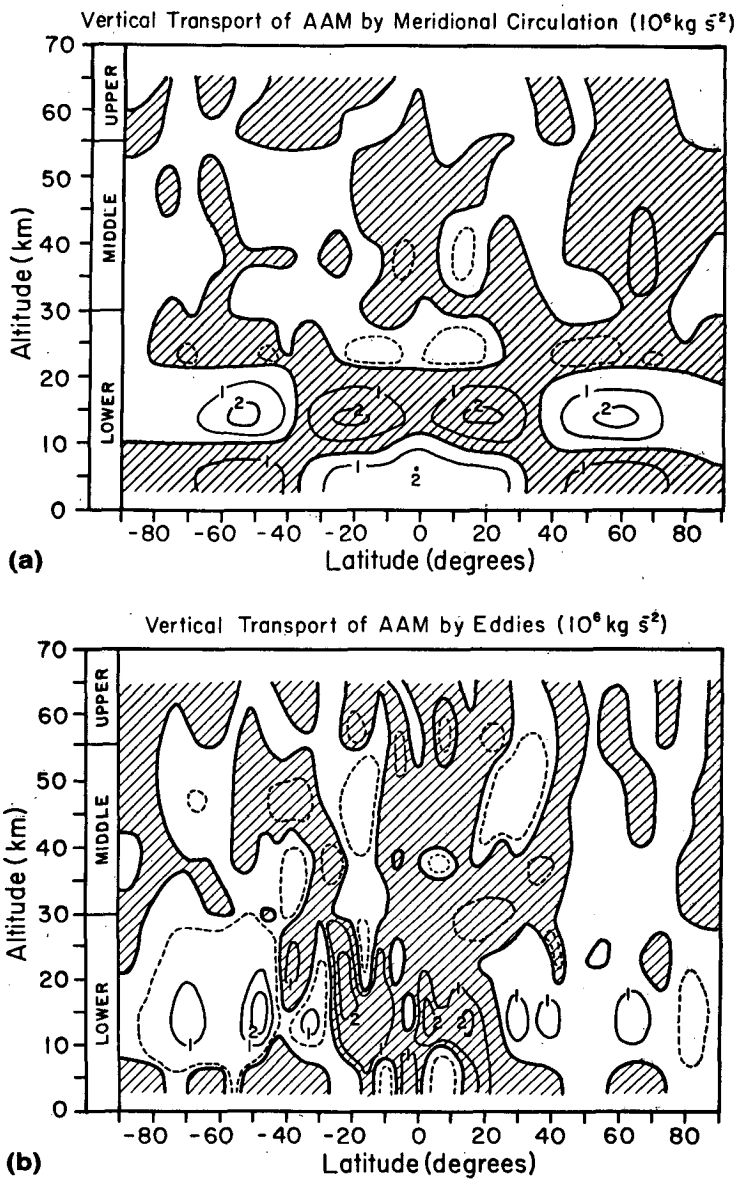

FIG. 9. Zonal mean vertical transport of absolute angular momentum by the meridional circulation (a) and eddies (b), as a function of altitude and latitude. Heavy line is zero contour, and shading indicates downward transport. Dashed contour is for 0.5×10^6 kg s^{-2}.

duced by such waves can be quite sensitive to the convective parameterization, the model resolution and numerics, and the atmospheric structure. In addition, the convection and the associated gravity waves in low and middle latitudes effectively redistribute the radiative heating/cooling in the middle atmosphere, thereby altering the forcing for the mean meridional circulation. Particularly significant is the low-altitude indirect cell in the middle atmosphere which nearly cancels out the net vertical momentum flux by the mean meridional circulation. Weakened upward transport by the mean meridional circulation and efficient downward transport by the low-latitude gravity wave modes may account for the weak superrotation obtained in the model.

e. Nature of the eddies

In Sections 4c and 4d, the model structure and circulation suggested differences in the role played by eddies in low and high latitudes. Near the equator, large eddy heating/cooling rates are correlated with zones of convective activity (Fig. 6c and 6d). The eddy heating/cooling is caused mostly by vertical flux

divergence, generally cooling the region near the convection in the lower atmosphere and heating the upper atmosphere. Most of the (area-weighted) vertical heat flux by eddies in the model occurs near the equator. The equatorial zone eddies are also solely responsible for the strong downward transport of angular momentum (Fig. 9b) and produce only weak poleward horizontal momentum transports. [when averaged over ±30° latitude (Fig. 8b)].

In contrast, the eddies at higher latitudes, correlated with the zonal jets, cause heating/cooling rates which are produced about as much by horizontal flux divergence as by vertical flux divergence. The vertical flux of angular momentum by these eddies is upward, but, like their vertical heat flux, confined in altitude rather than extending over the entire depth of the atmosphere like the equatorial eddy fluxes (Fig. 9b). These eddies also produce a systematic equatorward momentum transport. Further evidence is presented here to identify the equatorial eddies as vertically propagating gravity wave modes and the high-latitude eddies as the three-dimensional analog of barotropic eddies produced by instability of the zonal flow.

Fig. 10 shows the time-averaged, zonal mean energy conversion terms per unit mass, defined by Lorenz (1967) to indicate the sources and sinks of eddy kinetic energy (EKE): C_E is the conversion of EKE to eddy available potential energy (EPE) (baroclinic conversion) and C_{ZE} is the conversion of zonal kinetic energy (ZKE) to EKE (barotropic conversion). These two quantities, together with the parameterized dissipation, determine the global EKE budget. Local EKE budgets, however, are also influenced by the flux divergence of EKE by the circulation.

Fig. 10 shows that high and low latitudes in the lower atmosphere differ in their primary source of EKE. Near the equator (±20°), a pattern of strong EPE to EKE conversion extending into the middle atmosphere is correlated with the vertically alternating heating/cooling caused by convection (cf. Figs. 6d and 10a); this region is generally a region of weak EKE to ZKE conversion. The peak of the baroclinic conversion near 18–28 km in the lower atmosphere coincides with a peak in EKE and in the flux divergence of EKE. The flux divergence of EKE is produced primarily by vertical transport by the eddies themselves. These are characteristics of vertically propagating gravity waves (Holton, 1979); the correlation with the convective regions suggests that these gravity waves are stimulated by the temperature perturbations caused by convective adjustment in the statically stable middle atmosphere. The propagating waves are damped at the highest model level by strong radiative cooling (see Fig. 7).

The same correlation of heat transports, energy conversions and flux divergences with convection can also be seen at midlatitudes in the middle atmosphere, while opposite correlations are associated with the same three zones in the upper atmosphere near 60 km (Fig. 10a). This pattern of EPE to EKE conversion in the lower and the middle atmosphere and EKE to EPE conversion in the upper atmosphere with strong vertical fluxes of EKE in between is simply another way to indicate strong eddy vertical heat fluxes cooling the lower atmosphere and heating the upper atmosphere. The primary downward angular momentum flux by eddies in the model is also caused by these vertically propagating gravity waves stimulated by the convective adjustment.

At higher latitudes in the lower atmosphere, regions of barotropic conversion are associated with zonal jets (cf. Figs. 5c and 10b), suggesting that the source of EKE is the instability of the zonal flow. However, although baroclinic conversion is nearly zero at the jet core altitude, there is a region of baroclinic conversion *above* the jet center, which suggests that the eddy motions are more complicated than the horizontal, nondivergent motions required for barotropic conversion. Either the eddies are a consequence of a baroclinic instability of the zonal flow which also stimulates some barotropic conversion, or they are a consequence of a barotropic instability of the zonal flow, but are three-dimensional and stimulate some baroclinic conversion. The larger amplitude of C_E compared to C_{ZE} does not necessarily require the former interpretation since the magnitudes depend on both the strength of the eddy motions and the magnitudes of the temperature and momentum gradients;[10] hence, very weak motions in a massive atmosphere can produce large heat transports even with small temperature gradients. Laboratory experiments (Fultz *et al.*, 1959; Spence and Fultz, 1977; Hide, 1977) and modeling studies (Hunt, 1979; Williams and Holloway, 1982) argue against baroclinic instability of zonal flows at planetary rotation rates as slow as that in this model, but the nature of zonal flow instabilities in the slowly rotating regime has not been as thoroughly explored as those in the quasi-geostrophic regime. Detailed consideration of the relationships in geostrophic studies between the energy conversions and the eddy fluxes of momentum, geopotential, kinetic energy and heat, if they are not strongly changed by rotation effects, argues in favor of barotropic instability to explain the high latitude eddies.

Fig. 11 shows the zonal mean distribution of all the eddy-related quantities for a single model time step corresponding to the strongest zonal jet for which diagnostics were saved. Panel 1 shows the zonal wind with a jet centered at 10 km and 75° latitude. If this flow is barotropically unstable, then the absolute vorticity should have a local extremum associated with

[10] For instance, in Kuo's (1978) linear analysis, C_E is proportional to $v'p_y'$, i.e., to the product of a horizontal wind speed and a horizontal gradient.

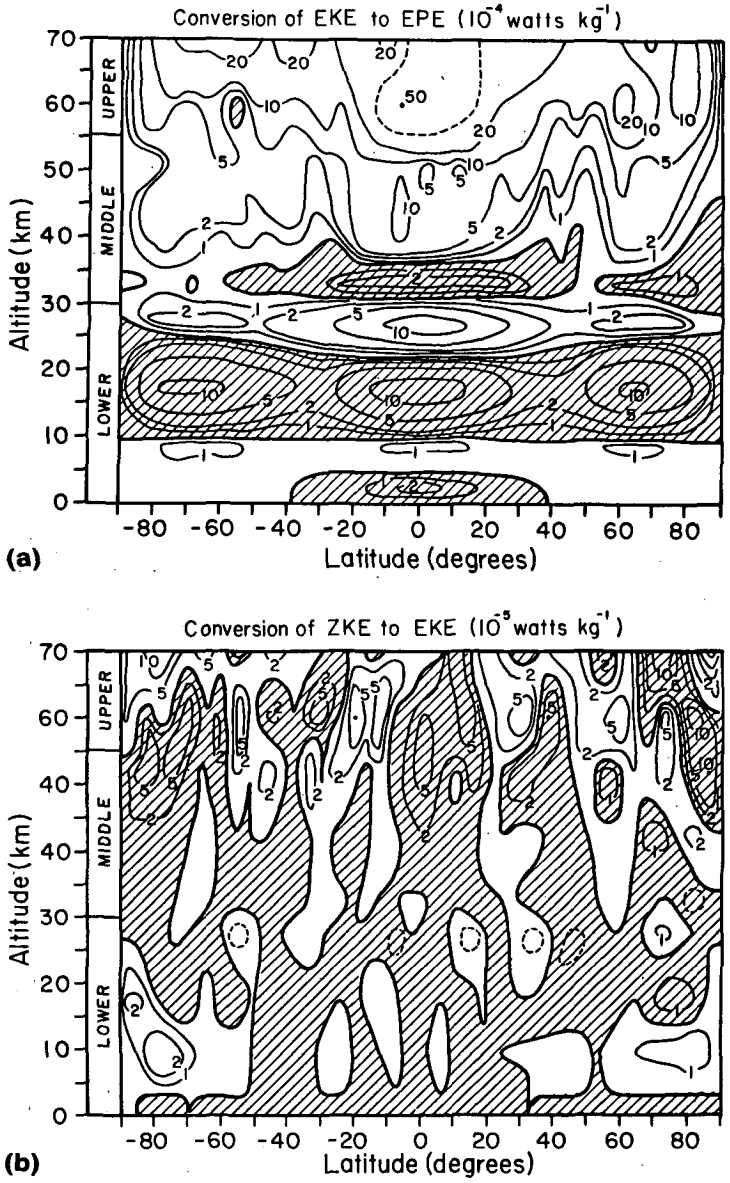

FIG. 10. Zonal mean energy conversion rates as function of altitude and latitude for (a) conversion of eddy kinetic to eddy potential energy and (b) of zonal kinetic to eddy kinetic energy. Heavy line is zero contour and shading indicates negative conversion rate. Dashed contour in (a) is for 30×10^{-4} W kg^{-1}. Dashed contour in (b) is for 0.5×10^{-5} W kg^{-1}.

the wind shear on one or both sides of the jet center (Kuo, 1949). The cross in Panel 1 shows the location of the minimum of vorticity in the hemisphere on the equatorward side of the jet at 67° latitude. Kuo's linear stability analysis (see Kuo, 1978)[11] shows that the instability should occur preferentially on the equatorward side of a westerly (positive) zonal jet with the zonal wavenumbers of the most unstable modes in the range of 2–4. Indeed, the EKE spectrum at 73° latitude is dominated by eddies of this wavenumber. Further, Panels 2, 3, 4, 11 and 13 exhibit a correlation of the jet center (zero vorticity) with the maximum of barotropic conversion and the minimum divergence of angular momentum and kinetic energy, and a correlation of the vorticity maximum with the minima of northward transport of angular momentum and kinetic energy. The latter two correlations are

[11] Kuo (1978) considers barotropic instability of tropical zonal flows where $f \approx 0$, but $\beta \neq 0$; however, he considers an order-of-magnitude range in β which does not seem to change the relationships discussed here.

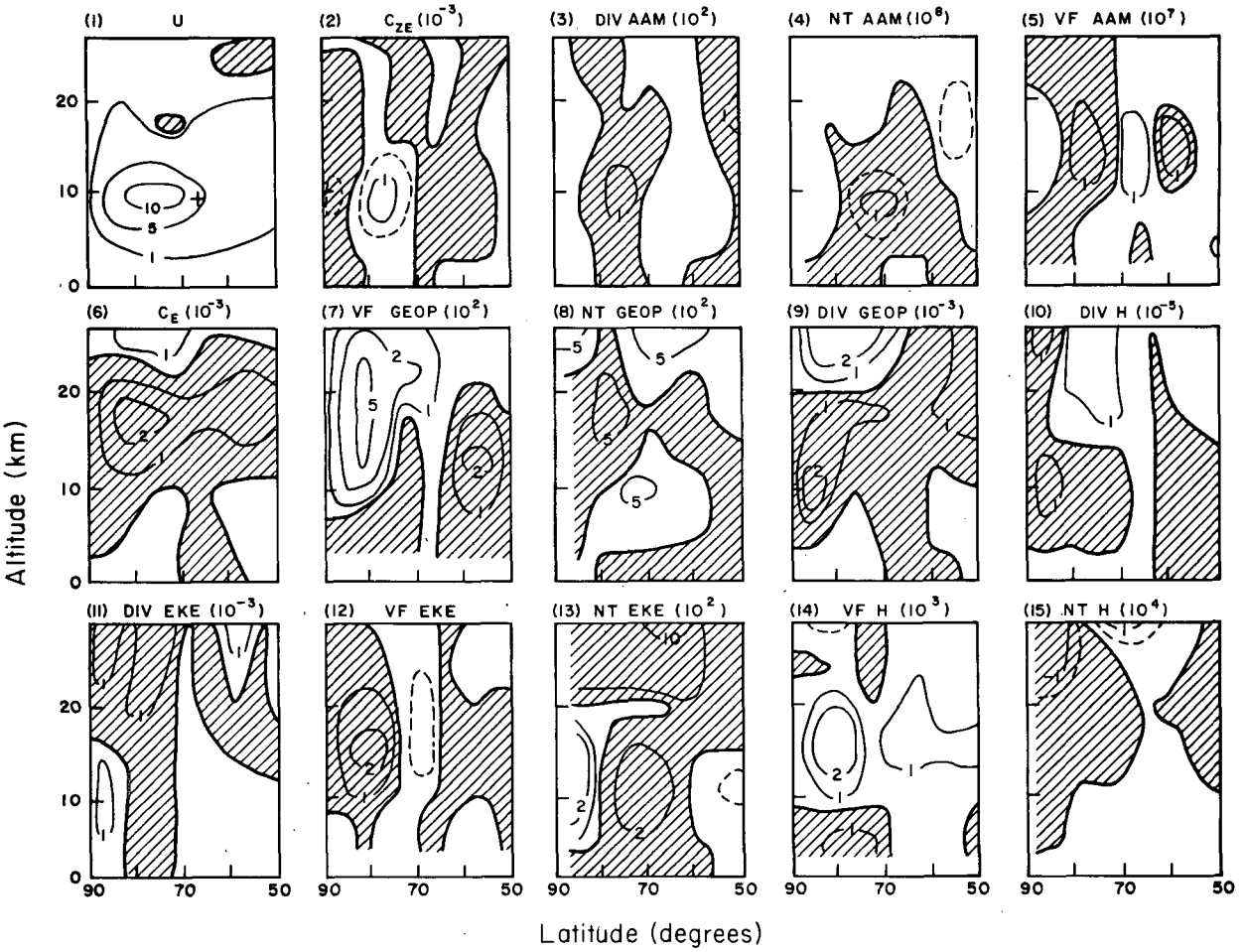

FIG. 11. Instantaneous zonal mean diagnostics for strongest zonal jet in lower atmosphere as a function of altitude and latitude. First row of contour plots, from left to right, represents the zonal wind speed (m s^{-1}), conversion rate from zonal to eddy kinetic energy (W kg^{-1}), eddy flux divergence of absolute angular momentum (m^2 s^{-2}), northward transport of absolute angular momentum by eddies (m^3 s^{-2}), and vertical flux of absolute angular momentum by eddies (kg s^{-2}). Second row of plots represents the conversion rate from eddy kinetic to eddy potential energy (W kg^{-1}), vertical flux of geopotential by eddies (W m^{-2}), northward transport of geopotential by eddies (m^3 s^{-3}), eddy flux divergence of geopotential (W kg^{-1}), and eddy flux divergence of heat (K s^{-1}). Third row of plots represents the total flux divergence of eddy kinetic energy (W kg^{-1}), total vertical flux of eddy kinetic energy (W m^{-2}), northward transport of eddy kinetic energy (m^3 s^{-3}), vertical flux of heat by eddies (W m^{-2}), and northward transport of heat by eddies (m^3 s^{-3}). Heavy lines are zero contours and shading indicates negative values. Dashed contours represent half of the lowest contour value.

predicted by linear barotropic instability analyses (Kuo, 1949, 1978), while the former correlations are shifted slightly compared to linear analysis by the finite-amplitude contribution of the vertical fluxes (Panels 5 and 12) of three-dimensional eddies. Kuo (1978) also shows that, in the presence of positive vertical wind shear, *three*-dimensional eddy motions convert EPE to EKE at the vorticity maximum and convert EKE to EPE on the poleward edge of the jet. This is consistent with the pattern of C_E shown below 10 km in Panel 6 (Fig. 11). Thus, all of the correlations in the model flow are consistent with those suggested by linear analyses of a barotropically unstable, vertically sheared zonal flow producing three-dimensional, rather than two-dimensional, eddy motions.

In contrast, the correlations expected[12] for baroclinically unstable flow are all contradicted by Fig. 11: 1) baroclinic conversion should be a minimum (maximum EPE to EKE convesion) on the poleward edge of the jet (Gall, 1976; Moura and Stone, 1976)–instead it is a double maximum on either side but *above* the jet center (Panel 6); 2) the minimum of C_E should correlate with the maxima of horizontal heat transport and divergence of momentum transport

[12] The calculations referred to here are all for quasi-geostrophic, i.e., rapidly rotating fluid flows and, thus, their applicability to a slowly rotating regime is uncertain. The similarity of the diagnostics to some features in Manabe and Mahlman's (1976) model lends support to the interpretation presented here.

(Gall, 1976; Moura and Stone, 1976; Simmons and Hoskins, 1978), which it does not (Panels 3, 6 and 15); 3) the minimum of C_E should correlate with the maxima of the vertical fluxes of heat and momentum (Gall, 1976; Simmons and Hoskins, 1978), which it does not (Panels 5, 6 and 14); and 4) all of these calculations exhibit a convergence of momentum into the region of maximum C_E (cf. Kuo, 1953), whereas Panels 3 and 6 show that the divergence is approximately zero in that region.

Thus, the region of baroclinic conversion above the jet is probably stimulated by the quasi-barotropic eddies in an analogous fashion to the stimulation of baroclinic conversions in Earth's stratosphere by upward propagating tropospheric eddies (Manabe and Mahlman, 1976). Figs. 9.2, 9.3, 9.5 and 9.6 in Manabe and Mahlman (1976) show a correlation between the minimum of C_E and the maxima of upward vertical flux of geopotential and of equatorward horizontal transport of geopotential in their model stratosphere. The same correlation is exhibited in this model in Panels 6, 7 and 8 (Fig. 11) near 20 km and 80° latitude, suggesting that vertical propagation of eddy energy from the jet region towards higher polar altitudes is responsible for the baroclinic conversions aloft.

The horizontal transport of angular momentum by these three-dimensional "barotropic" eddies is further elucidated in Fig. 12. The upper curves show that the equatorward transport of momentum by the eddies is up the absolute angular momentum gradient. Such transport shifts relative angular momentum equatorward, increasing the gradient of absolute angular momentum at lower latitudes (illustrated by the middle curves in Fig. 12). This shift produces a zonal flow with an angular momentum gradient more like that of solid rotation (analogous to the planetary angular momentum gradient shown). The bottom curves show that this type of momentum transport is equivalent to transporting vorticity down its gradient to produce a vorticity distribution more like that of solid rotation. Thus, the three-dimensional eddy motions, associated with the shear instability of the zonal jet in this model, influence the angular momentum distribution of the model circulation in a fashion analogous to two-dimensional eddies. Further, since their heat transport is much less efficient than their momentum transport, as evidenced by a time-averaged Prandtl number[13] of ~ 10, these eddies can play the role in the momentum budget proposed by Rossow and Williams (1979).

All of this discussion is based on theoretical studies of eddies in the rapidly rotating dynamic regime,

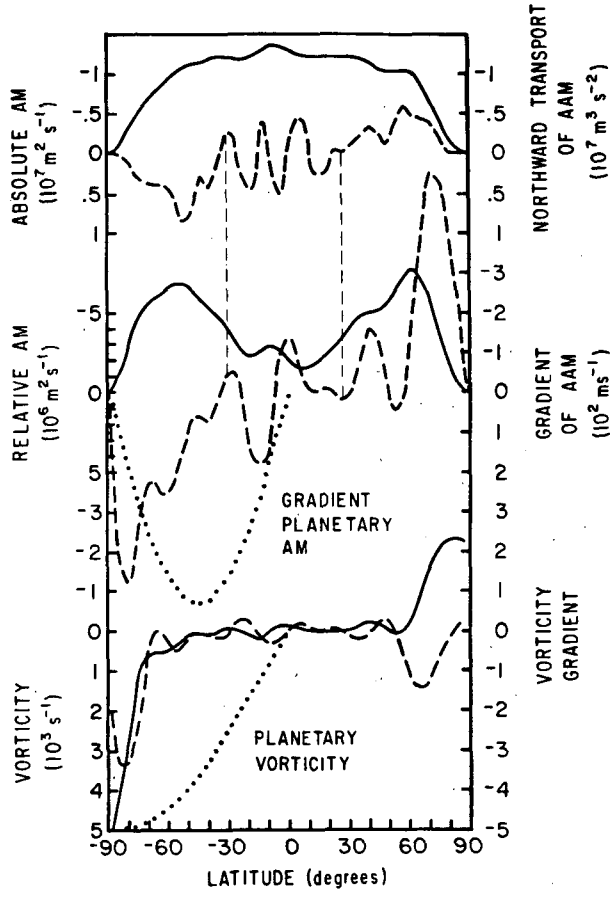

FIG. 12. Zonal mean quantities relating to eddy angular momentum transport for model level 8, as a function of latitude. Solid lines refer to the left scale and dashed lines to the right scale. Quantities shown are absolute angular momentum, northward transport of absolute angular momentum by eddies, relative angular momentum, latitudinal gradient of absolute angular momentum, latitudinal gradient of planetary angular momentum (arbitrary units), absolute vorticity, latitudinal gradient of vorticity and the vorticity corresponding to the planetary (solid body) rotation (arbitrary units). The sign convention used in this figure is for retrograde zonal flow on a planet rotating in the retrograde direction.

which may not adequately describe the three-dimensional eddies occurring in the slowly rotating dynamic regime. The conclusions reached here are thus tentative, at best.

5. Discussion

This section concerns the ways in which the three-dimensional circulation of this model resembles or differs from the behavior exhibited by simpler linearized or two-dimensional models studied previously. Analogous behavior suggests that the processes isolated for study in simpler theoretical models have some general importance to the general three-dimensional circulation of a slowly rotating atmosphere, but differences suggest that much more work is required

[13] The Prandtl number is estimated by comparing the ratio of the horizontal eddy momentum transport and the equator-to-pole angular momentum gradient to the ratio of the horizontal eddy heat transport and the equator-to-pole heat content gradient.

to understand this dynamic regime. There are also some qualitative similarities between the model circulation and observations of Venus, which suggest possible interpretations of the Venus data; however, large quantitative differences make these interpretations speculative.

a. Lower atmosphere thermal structure

Stone (1974) derived scale relationships for the equilibrium horizontal and vertical temperature contrasts and mean meridional and vertical velocities using a linearized, Boussinesq, two-dimensional model in which only the mean meridional circulation transports heat and momentum. Stone's solution to the equations of motion for a statically unstable radiative equilibrium state, as in the model lower atmosphere, gives

$$\frac{A}{B} = \frac{B_e}{|A_e|}, \tag{15}$$

where A and A_e are the dimensionless vertical temperature lapse rates and B and B_e the dimensionless horizontal temperature gradients for dynamic and radiative equilibrium, respectively [see Stone (1974) for definitions]. With Pollack and Young's (1975) radiative equilibrium vertical profile (Fig. 2) and the simple latitude dependence assumed in the model (see Section 3d), $|A_e| \approx 0.3$ and $B_e \approx 1.3$, which gives $A/B \approx 4$. If the equilibrium temperature contrasts in the model are averaged over the whole lower atmosphere (two scale heights), then $A/B \approx 0.09/0.003 \approx 30$; but, if the contrasts are averaged only over the lowest circulation cell (<1 scale height), then $A/B \approx 0.08/0.005 \approx 16$. If the model values of A, A_e, B and B_e are also used in Stone's expressions for the mean meridional velocity $\bar{v}$ and the relaxation time constant t^* for the vertical temperature gradient, then the calculated $\bar{v}$ is ~ 10 times larger and $t^* \sim 20$ times smaller than obtained in the model.

Most of these differences can be explained by considering both the heat and momentum budgets of these two models, illustrating a key point: understanding of realistic mean meridional circulations cannot be obtained by neglecting important parts of *either* budget (cf. Held and Hou, 1980; Taylor, 1980). Stone's (1974) model momentum equations neglected all of the terms on the right of (1), except for the pressure gradient term and the mean meridional contribution to the advective terms. Specifically, he neglected all eddy fluxes and all three-dimensional effects, as well as surface drag and dissipation by smaller scale eddies. In the model, these terms are all comparable[14] so that the pressure gradient implied by the equilibrium value of B is partially offset by these other effects and causes weaker meridional circulations than predicted by Stone's (1974) expressions. In other words, the mean meridional circulation of a realistic three-dimensional circulation can be much less efficient than Stone's scaling analysis assumes. If the observed B and $\bar{v}$ are used to rescale Stone's expression, then his results predict $A \approx 0.03$ and $B \approx 0.007$, not too different from the model values. Thus, differences between atmospheric and model momentum budgets, especially regarding the importance of eddies and parameterized fluxes, could radically alter conclusions concerning the relation between meridional circulations and temperature contrasts (see, e.g., Taylor, 1980).

Stone's study was concerned with whether the mean, large-scale convective motions could maintain statically stable conditions instead of invoking small-scale convection as usually assumed. In the model presented here, both processes are allowed to occur; but the resulting circulation is complicated further by the propagating gravity waves stimulated by the convection. The combined convective and gravity wave heat fluxes produce a static stability larger than that maintained by the mean meridional circulation alone ($A \approx 0.09$ vs. $A \approx 0.03$), if Stone's scaling analysis is correct. The "extra" vertical heat flux at equatorial latitudes also enhances the poleward heat transport by the upper branch of the mean meridional circulation, which explains a smaller horizontal gradient ($B \approx 0.003$ vs. $B \approx 0.007$). However plausible these statements are, the interplay between the convection and mean meridional circulation is much more complicated as evidenced by the concentration of convection into a latitude zone narrower than that destabilized by radiation (Figs. 6a and 6d) and by the triple-maxima structure in the low-latitude cooling of the meridional circulation (Fig. 6b). The simple question of which dynamic mode controls vertical heat fluxes probably has a complex answer which depends more on the physics of radiation and convection than on planetary rotation rate.

The model results exhibit no significant horizontal heat flux by eddies, despite the exaggeration of horizontal differential heating. Thus, heat transport from equator to pole by the mean meridional circulation seems sufficient to balance differential solar heating and produce a nearly barotropic atmosphere in a slowly rotating atmosphere. The magnitude of the horizontal temperature gradient which results from a balance between radiation and the meridional heat transports is larger in a three-dimensional circulation than predicted by Stone (1974), as discussed above, because the momentum balance involves important eddy and three-dimensional (cyclostrophic) contributions neglected by Stone. Although eddy motions caused by other processes (as discussed in Section 4) can produce weak heat transports when small tem-

[14] Averaged over the lowest circulation cell, the cyclostrophic term is ~30% of the pressure gradient term, the mean meridional momentum advection is ~10%, the eddy momentum transport is ~20%, and the surface drag is ~10% [see Eq. (1)]. Parameterized horizontal eddy diffusion is only ~1% of the pressure gradient.

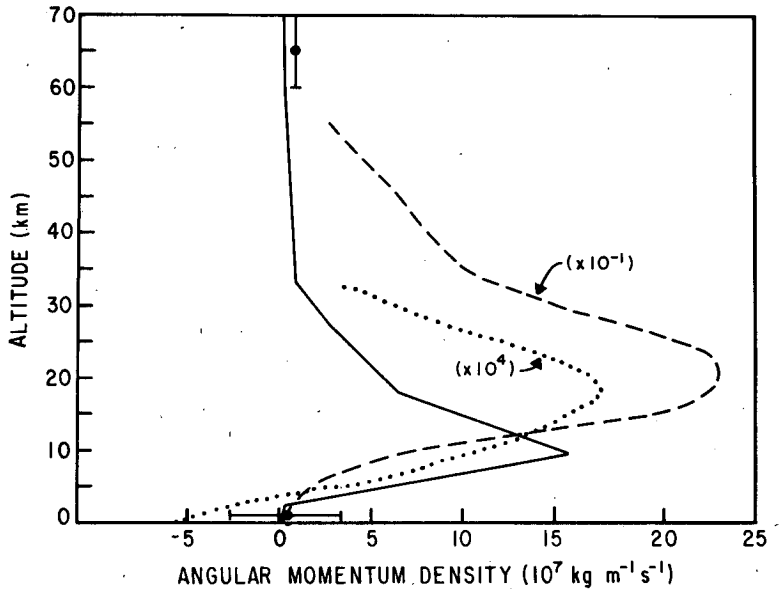

FIG. 13. Horizontally averaged angular momentum density as a function of altitude for the model (solid), Venus (dashed) and Earth (dotted). Plotted values for Venus are observed values at 30°S for two longitudes, which represents an approximation to the horizontal average of all the Pioneer Venus probe observations (Schubert *et al.*, 1980). Earth values, calculated from data of Oort and Rasmusson (1971), are plotted with twice as large a vertical scale for comparison with the other curves. The point with an error bar near 70 km represents the winds observed by the Pioneer Venus Orbiter Cloud Photopolarimeter (OCPP) (Rossow *et al.*, 1980). The error bar on the Venus profile near the surface reflects the uncertainty in probe wind measurements (Counselman *et al.*, 1980).

perature gradients are present, baroclinic instability, like that in Earth's midlatitudes, probably plays no role in the general ciculation of a slowly rotating atmosphere. Williams and Holloway (1982) also obtain this result with a slowly rotating general circulation model of Earth.

Observations of the lowest 30 km of Venus' atmosphere are consistent with a nearly neutral static stability and horizontal temperature contrasts $\leqslant 10$ K (Marov, 1978; Seiff *et al.*, 1980) and set upper limits on meridional wind speeds of ~ 2 m s^{-1}. Uncertainties in these measurements, as well as those of the radiative fluxes, are large; consequently, evaluation of the relative importance of small-scale convection and the mean meridional circulation to determining the static stability on Venus is not yet possible.

b. Lower atmosphere momentum distribution

In the model the vertical structure of the meridional circulation is correlated with the vertical distribution of total heating/cooling caused by radiation, convection and eddies (Fig. 7). Similar sensitivity of the meridional circulation to the vertical distribution of heating is exhibited in other models of Venus (Kalnay de Rivas, 1973) and of Earth (Schneider and Lindzen, 1977). If convection and eddies do not significantly redistribute the net heating/cooling on Venus, then net flux measurements from Pioneer Venus, which show net radiative heating/cooling extending over the lowest 20 km (Tomasko *et al.*, 1980a; Suomi *et al.*, 1980), imply a single direct meridional circulation cell in this region. A hint that this might be the case is given by Fig. 13 which shows the global mean vertical distribution of angular momentum on Venus and Earth and in the model. One feature common to all three distributions is the concentration of westerly[15] momentum away from the surface. The correspondence of this feature with the poleward branch of the direct mean meridional circulation on Earth and in the model suggests the same correspondence on Venus, that is, a Hadley circulation in the lower atmosphere extending over the lowest 20–25 km.

The momentum distributions shown in Fig. 13 also indicate an important difference between Earth and both the model and Venus; namely, the mean relative angular momentum is easterly at the surface on Earth, but nearly zero for Venus and the model. This difference, together with the concentration of momentum in the poleward branch of the direct circulation cell, can be understood using the zonal equa-

[15] Westerly refers to the direction of planetary rotation.

tion of motion in flux form for a steady state equilibrium:

$$\nabla \cdot (\overline{\rho M}\,\overline{\mathbf{V}}) + \nabla \cdot (\overline{\rho M' \mathbf{V}'}) + \bar{T} = 0, \qquad (16)$$

where $M = ua\cos\theta + \Omega a^2 \cos^2\theta$ is the total angular momentum, the first term represents the momentum flux divergence by the zonal mean circulation, the second represents that by the eddies, and $\bar{T}$ represents the surface torque on the atmosphere (the overbar represents a zonal average). Many numerical models and analytic studies parameterize the eddy contribution to (16) as molecular diffusion, but planetary-scale eddies do not necessarily behave in this fashion as the model results presented here illustrate (see, also, Plumb, 1979). Indeed, the difference between eddy momentum transports in the model and on Earth is responsible for the difference in the mean angular momentum at the surface.

Consider the momentum distribution produced by a Hadley circulation in frictional contact with a rotating solid suface and in steady-state equilibrium. Since the total atmospheric angular momentum is not changing, the horizontally averaged torque

$$\hat{T} = \int \bar{T} \cos\theta d\theta = 0. \qquad (17)$$

Since advection by the Hadley circulation in (16) conserves angular momentum, an equator-to-pole cell produces westerlies at higher latitudes and easterlies at lower latitudes, as Hadley first pointed out (Lorenz, 1967). The usual formulation of surface drag makes the surface torque proportional to $u^2 \cos\theta$, so that for $\hat{T} = 0$ in balance with a Hadley circulation, the surface westerly wind magnitude must be roughly $(\cos\theta)^{-1}$ times the easterly magnitude. On the other hand, the horizontally averaged angular momentum

$$\hat{M} = \int \bar{M} \cos\theta d\theta, \qquad (18)$$

can only be zero if the westerly magnitude is approximately $(\cos\theta)^{-2}$ times the easterly magnitude; hence, $\hat{M} < 0$, in this case.

Now, if the eddy motions serve to transport angular momentum *downgradient,* the maximum of the *total* angular momentum must be on the surface at the equator (see Held and Hou, 1980). Consequently, the eddy momentum flux is upward and poleward strengthening the westerly flow aloft in higher latitudes (cf. Kuo, 1953) and shifting the vertical distribution of *relative* angular momentum towards that shown for Earth in Fig. 13, with a maximum aloft and $\hat{M}$ even more negative at the surface. On Earth the Hadley circulation is actually confined near the equator ($\leqslant 30°$) and baroclinic eddies, on average, transport angular momentum poleward (downgradient, horizontally) (Oort and Rasmusson, 1971) out of this region. Thus, the Hadley circulation region is a net source of positive momentum, i.e., $\hat{T} > 0$, requiring a broader zone of surface easterlies and producing more concentration of momentum in the westerly jet (see Held and Hou, 1980; Taylor, 1980).

In the model, the Hadley circulation extends from equator to pole and the quasi-barotropic eddies transport momentum *upgradient* (horizontally) toward the equator (Fig. 12). These eddies weaken the westerly and easterly flows, i.e., they weaken the gradient of angular velocity, in contrast to the baroclinic eddies on Earth which strengthen the angular velocity gradient. Since the upward branch of the Hadley circulation now carries up more momentum than the downward branch carries down, the maximum of *total* angular momentum moves upward off the surface (Gierasch, 1975), which also produces a maximum of *relative* angular momentum aloft (cf. Fig. 7, Schubert *et al.,* 1980). Such a result was even produced in a model of a rapidly rotating atmosphere using very strong upgradient diffusion (Hunt, 1973). Furthermore, the eddy transport of momentum toward the equator near the surface broadens the region of surface westerlies and narrows the region of easterlies, so that $\hat{M}$, with $\hat{T} = 0$, shifts towards zero.[16]

Fig. 14 shows that the angular velocity gradient in the lower atmosphere of Venus is nearly zero, a distribution which cannot be produced by a thermally direct Hadley circulation alone, but is consistent with strong upgradient momentum transport. The qualitative features of the angular momentum distribution on Venus, exhibited in Figs. 13 and 14, are suggestive of the interaction between a thermally driven meridional circulation and quasi-barotropic eddies like that exhibited in this model, although these features do not uniquely determine the source of eddy motions on Venus. Barotropic instability of the zonal flow (Rossow and Williams, 1979) is only one possibility.

The latitudinal extent of a thermally driven Hadley circulation may well depend on the eddy momentum transports as well. Held and Hou (1980) and Taylor (1980) have demonstrated such a dependence in models of Earth's meridional circulation; in some cases, they obtain Hadley cells extending to the pole even in a rapidly rotating atmosphere. On the other hand, the mean meridional circulation at the level of solar absorption, obtained by Kalnay de Rivas (1973, 1975) is composed of a thermally direct Hadley cell and a weak indirect polar cell when horizontal eddy momentum transports are neglected. The mean meridional circulation obtained in this model exhibits single direct (and indirect) cells extending from equator to pole. Thus, the latitudinal extent of the thermally direct circulation cells in simple models may not be a simple function of planetary rotation rate,

[16] In the model, the strong downward momentum flux at the equator by eddies produces a region of surface westerlies to act as a sink of momentum; the easterlies at middle latitudes strengthen somewhat to compensate.

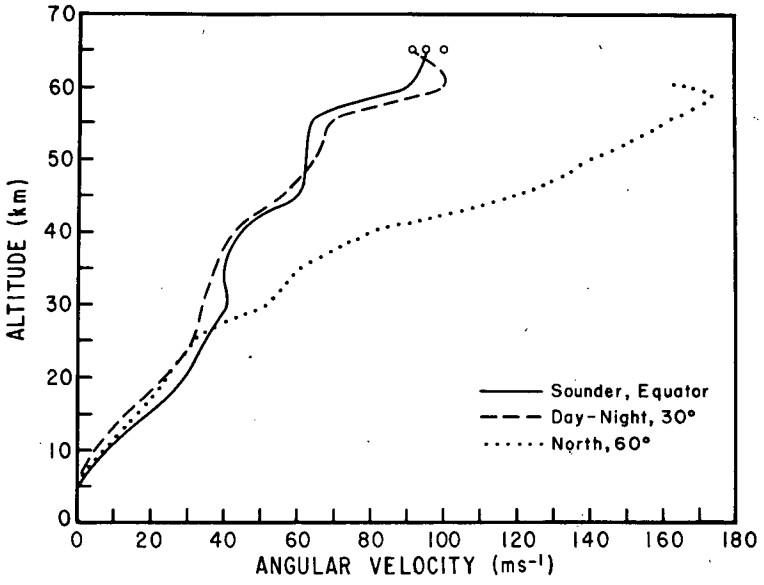

FIG. 14. Angular velocity as a function of altitude and latitude from Pioneer Venus probe measurements (Counselman *et al.*, 1980). Values shown are zonal velocities scaled by $(\cos\theta)^{-1}$. The three open circles are wind measurements for the same latitudes (except for 60° value from Southern Hemisphere) from Pioneer Venus OCPP cloud-tracked winds (Rossow *et al.*, 1980).

but rather may depend more on parameterizations of eddy momentum processes (cf., Kalnay de Rivas, 1973, 1975; Hunt, 1973, 1979; Held and Hou, 1980; Taylor 1980). The nearly barotropic thermal state produced by the mean meridional circulation in slowly rotating atmospheres may insure that eddy momentum transports generally become similar to those in this model, regardless of how the eddies are produced (cf. Williams and Holloway, 1982). Hunt (1979) notes a switch of eddy momentum transport from the downgradient to the upgradient direction as planetary rotation is decreased. Consequently, equator-to-pole Hadley circulations will be a general feature of slowly rotating atmospheres.

c. *Upper atmosphere circulation*

The observed vertical distribution of angular momentum on Venus (Fig. 13) points to a major difficulty in understanding the cause of the strong zonal flow near cloud tops: the amount of angular momentum in the lower atmosphere is more than 20 times as large as that associated with the strong zonal winds at cloud levels, implying that whatever process is responsible for transporting angular momentum to the cloud-top region from the lower atmosphere is *very inefficient*. Hence, numerical modeling studies of the momentum budget in the lowest 6–10 scale heights of Venus' atmosphere will be extremely sensitive to model simplifications and parameterizations which distort, even slightly, the dynamical vertical momentum transports. In particular, *ad hoc* parameterizations of small-scale eddy transport may overwhelm weak vertical transports by other explicit motions. The particular characteristics of the convection parameterization used in this model, for example, may have prevented the build-up of large zonal flows in the upper atmosphere; other parameterizations including momentum transport (cf. Hansen *et al.*, 1983) may produce different results. On the other hand, the presence of strong zonal flows in other models may only be a consequence of the form of parameterization chosen for small-scale motions (Rossow *et al.*, 1979; cf. results in Hunt, 1973).

The model results presented here clearly confirm that the operation of a process like that proposed by Gierasch (1975) and Rossow and Williams (1979) can produce mean westerly (in direction of rotation) momentum *at all altitudes* in a fully three-dimensional circulation. The model does not, however, produce a zonal flow as strong as observed on Venus, so that the efficiency of this process cannot be evaluated. However, the model dynamics are general enough to conclude that the interaction of quasi-barotropic eddies and the thermally driven meridional circulation causes *some* superrotation of the whole atmosphere on slowly rotating planets.

When Gierasch (1975) proposed that meridional circulations transport momentum upward on average, he envisioned the thermally driven mean meridional circulation as a single deep Hadley circulation. Model results and observations of winds and solar absorption on Venus suggest that the thermally driven mean meridional circulation there is probably multicellular. Nevertheless, this model demonstrates that such multicellular meridional circulations can

still transport angular momentum from the surface all the way to the cloud tops. This can be explained by decomposing the complete meridional circulation into a primary single-cell mode and other modes of increasing vertical wavenumber (like vertical Fourier analysis): despite the predominance of kinetic energy in modes with wavenumbers > 1 in the flow, the primary mode momentum flux may still exceed the sum of the fluxes of the other modes resulting in a net transport from the surface to the cloud tops. Fig. 13 shows that the net transport on Venus need not be very strong.

When Rossow and Williams (1979) proposed that quasi-nondivergent, quasi-barotropic eddies are responsible for the horizontal momentum transport required in Gierasch's model for the strong zonal flow, they argued that, although these eddies might have vertical motion components, hence transport heat, these divergence effects are very weak, second-order effects. The model results confirm that this type of eddy motion is possible. Although the large-scale eddies associated with the zonal jets do exhibit vertical motions which cause horizontal heat transport, the effective Prandtl number of the eddies is much larger than unity, while that of the mean meridional circulation is of order unity. These eddies can then be said to be *quasi*-barotropic as proposed by Rossow and Williams (1979); however, more study of this type of three-dimensional eddy motion is needed.

Whatever the process responsible for supplying angular momentum to cloud levels on Venus, a balancing removal process remains to be identified. All of the theoretical models use some *ad hoc* vertical momentum flux to balance the supply process. In this model, momentum is removed from the upper atmosphere by the small-scale propagating gravity waves stimulated by convection in the equatorial zone. Another possibility is that the planetary-scale tidal modes (which are neglected in this model), excited either near the surface (Dobrovolskis and Ingersoll, 1980) or at cloud levels (Fels, 1977), could transport momentum out of cloud levels. This is the reverse of the "moving flame" process proposed by Schubert and Whitehead (1969). Understanding the dynamics of cloud levels on Venus clearly requires careful study of *nonlinear* wave dynamics problems for deep atmospheres, especially for basic states with strong horizontal and vertical wind shears (see, especially, Andrews and McIntyre, 1976).

6. Summary

a. Can the mean meridional circulation provide the dominant vertical and horizontal heat flux in a massive, slowly rotating atmosphere?

Comparison between the model and Stone's (1974) scaling shows good agreement if the efficiency of the mean meridional circulation is reduced. In other words, the effects of eddy momentum transports and the zonal flow (through the cyclostrophic term) in a three-dimensional, slowly rotating circulation reduce the effective pressure gradient driving the meridional circulation. On Earth, both the geostrophic effect away from the equator and baroclinic eddy momentum fluxes are also important, but they may have opposite effects on the pressure gradient driving the tropical Hadley circulation (Taylor, 1980). Despite the lower efficiency, the mean meridional circulation maintains a nearly barotropic thermal state and horizontal eddy heat fluxes are negligible; that is, the meridional circulation probably provides the dominant horizontal heat transport in slowly rotating atmospheres.

Although the mean meridional circulation apparently can provide enough vertical heat flux to stabilize the atmosphere against radiation, this fact does not preclude the occurrence of some small-scale convection. The model displays a complicated interaction between these two dynamic modes which deserves further study: the horizontal distribution of convection seems to be controlled by the mean meridional circulation (cf. Figs. 4, 6b and 6d), while the vertical structure of the meridional circulation seems under the influence of the convection and associated eddies (Fig. 7). The partitioning of vertical heat fluxes between these two dynamic modes, as well as the presence of additional transports by other eddies, is probably more dependent on the details of the radiative forcing for a particular atmosphere than on the planetary rotation rate. These model results suggest that, while the meridional circulation provides important vertical heat transports, other processes, such as small-scale convection, can also play comparable roles.

b. What determines the vertical and horizontal structure of the mean meridional circulation?

The model results suggest that the vertical structure is determined by the vertical distribution of the total heating produced by radiation, convection and eddies near the equator. However, near the surface, momentum considerations may play a role if boundary layer processes cause strong drag effects. These results, together with those from other models, indicate that the horizontal structure is dependent on the nature of the horizontal eddy momentum transports; but that slowly rotating atmospheres probably contain equator-to-pole meridional circulation cells. However, such simple answers are misleading descriptions of what is a complex coupling between the momentum and heat budget equations; the complete answer to this question must lie in consideration of both budgets. Domination of one particular aspect of the circulation may be determined more by the particular

properties of each atmosphere than by the planetary rotation rate.

c. Can the mean meridional circulation transport momentum over large vertical distances?

These model results confirm Gierasch's (1975) hypothesis in a fully three-dimensional circulation: the meridional circulation can transport momentum upward over many scale heights, even if the circulation is vertically divided into many cells.

d. Do some eddy motions behave as if they were barotropic, two-dimensional motions?

The model results demonstrate this possibility, suggested by Rossow and Williams (1979), in a fully three-dimensional circulation. The existence of such motions is probably more dependent on the fact that, for a slowly rotating atmosphere, the mean meridional circulation maintains a nearly barotropic thermal structure. Consequently, large-scale eddies produced by other mechanisms may also behave like the eddies in this model. The results of Williams and Holloway (1982) seem to demonstrate this point. The properties of such three-dimensional, quasi-barotropic eddies have not been studied in the slowly rotating dynamical regime.

e. What about Venus?

The model circulation does not have as strong a superrotation as observed on Venus. Consequently, the heat transporting efficiency of the meridional circulation, especially in the upper atmosphere, is probably less on Venus than in the model because of the cyclostrophic term in the momentum equations. In the lower atmosphere, where the zonal flow on Venus is only 3–5 times stronger than in the model, the mean circulation is still probably composed of equator-to-pole mean meridional circulation cells producing a quasi-barotropic thermal state. As a consequence, large-scale eddy motions would behave analogously to two-dimensional eddy motions producing equatorward momentum fluxes and triggering net upward momentum transport by the mean meridional circulation. Thus, some superrotation of the whole atmosphere on Venus, caused by these processes, seems likely; but application of these results to Venus is not possible in detail, both because observations do not serve to define the critical processes adequately and because theoretical understanding of many processes in this dynamic regime is not available. With regard to the momentum balance of the upper atmosphere of Venus, extreme care in modeling convection and other eddy vertical transports is required before modeling results can be accepted. The focus of future work should be on the processes producing eddy motions and governing their behavior in slowly rotating atmospheres like that on Venus.

Acknowledgments. This paper is based on calculations performed while the author was part of the Geophysical Fluid Dynamics Program of Princeton University and NOAA Geophysical Fluid Dynamics Laboratory. The model is a modification of a model used by the GFDL Experimental Long Range Forecasting Group headed by K. Miyakoda. Vital assistance in making the modifications was given by W. Stern, R. Hovanec and C. Gordon. G. Williams at GFDL gave me much encouragement and advice throughout this project. Conversations with A. Del Genio, S. Fels, P. Gierasch, P. Stone and L. Travis helped form my ideas for this paper. Assistance in preparing the figures was given by N. Kane; graphics were done by L. Del Valle and J. Mendonza. Typing was done by B. Duckett and D. Smith.

APPENDIX

List of Symbols

a	planetary radius
f	Coriolis frequency [$=2\Omega \sin\theta$]
g	acceleration of gravity
$\hat{\mathbf{k}}$	unit vector perpendicular to sigma coordinate surfaces
t	time
C_D	bulk surface drag coefficient
C_p	atmospheric heat capacity per unit mass at constant pressure
D	horizontal wind divergence [$=\nabla_H \cdot \mathbf{V}$]
$\mathbf{F}_m$	parameterized acceleration due to unresolved eddy motions
F_T	parameterized heating rate due to unresolved eddy motions
P	atmospheric pressure
P_s	surface pressure
Q_{rad}	net radiative heating rate
R	universal gas constant divided by mean molecular weight
T	atmospheric temperature
T^*	global mean radiative equilibrium temperature
T_{eq}	local radiative equilibrium temperature
$\mathbf{V}$	three-dimensional wind velocity.
Y_L^m	surface spherical harmonic function
α	filter factor in time stepping routine
ζ	vertical component of vorticity [$=\hat{\mathbf{k}} \cdot \nabla_H \times \mathbf{V}$]
η	vertical heat flux in turbulent surface boundary layer
θ	latitude defined with positive values in hemisphere with positive planetary rotation vector
Θ	potential temperature
ν	coefficient of horizontal eddy viscosity
ρ	atmospheric mass density
σ	vertical model coordinate [$=P/P_s$]

$\dot{\sigma}$ vertical velocity in sigma coordinates
τ surface stress on first model level
τ_{rad} radiative time constant
ω vertical velocity in pressure coordinates
Γ dry adiabatic temperature lapse rate $[=g/C_p]$
Φ geopotential
Ω planetary rotation rate
∇_H horizontal gradient operator.

REFERENCES

Allen, C. W., 1973: *Astrophysical Quantities.* Athlone Press, 140–141.

Andrews, D. G., and M. E. McIntyre, 1976: Planetary waves in horizontal and vertical shear: The generalized Eliassen–Palm relation and the mean zonal acceleration. *J. Atmos. Sci.*, **33**, 2031–2048.

Bourke, W., B. McAvaney, K. Puri and R. Thurling, 1977: Global modeling of atmospheric flow by spectral methods. *Methods in Computational Physics,* Vol. 17, J. Chang, Ed., Academic Press, 267–324.

Chalikov, D. V., A. S. Monin, A. S. Safray, V. G. Turikov and S. S. Zilitinkevich, 1975: Numerical simulation of the general circulation of the Cytherean lower atmosphere. *Icarus,* **26**, 178–208.

Counselman, C. C., S. A. Gourevitch, R. W. King and G. B. Loriot, 1980: Zonal and meridional circulation of the lower atmosphere of Venus determined by radio interferometry. *J. Geophys. Res.*, **85**, 8026–8030.

Del Genio, A. D., and W. B. Rossow, 1982: Temporal variability of ultraviolet cloud features in the Venus stratosphere. *Icarus,* **51**, 391–415.

Dickinson, R. E., and E. C. Ridley, 1975: A numerical model for the dynamics and composition of the Venusian thermosphere. *J. Atmos. Sci.*, **32**, 1219–1231.

Dobrovolskis, A. R., and A. P. Ingersoll, 1980: Atmospheric tides and the rotation of Venus. I. Tidal theory and the balance of torques. *Icarus,* **41**, 1–17.

Douglas, H. A., P. J. Mason and E. H. Hinch, 1972: Motion due to a moving internal heat source. *J. Fluid Mech.*, **54**, 469–480.

Fels, S. B., 1977: Momentum and energy exchanges due to orographically scattered gravity waves. *J. Atmos. Sci.*, **34**, 499–514.

——, and R. S. Lindzen, 1974: The interaction of thermally excited gravity waves with mean flows. *Geophys. Fluid Dyn.*, **6**, 149–191.

Fultz, D., R. Long, G. Owens, W. Bohen, R. Kaylor and J. Weil, 1959: *Studies of Thermal Convection in a Rotating Cylinder with some Implications for Large-Scale Atmospheric Motions. Meteor. Monogr.*, No. 21, Amer. Meteor. Soc., 104 pp.

Gall, R., 1976: A comparison of linear baroclinic instability theory with the eddy statistics of a general circulation model. *J. Atmos. Sci.*, **33**, 349–373.

Gierasch, P. J., 1975: Meridional circulation and the maintenance of the Venus atmospheric rotation. *J. Atmos. Sci.*, **32**, 1038–1044.

——, R. M. Goody and P. H. Stone, 1970: The energy balance of planetary atmospheres. *Geophys. Fluid Dyn.*, **1**, 1–18.

Goody, R. M., and A. R. Robinson, 1966: A discussion of the deep circulation of the atmosphere of Venus. *Astrophys. J.*, **146**, 339–353.

Gordon, C. T., and W. F. Stern, 1982: A description of the GFDL global spectral model. *Mon. Wea. Rev.*, **110**, 625–644.

Hansen, J. E., G. Russell, D. Rind, P. Stone, A. Lacis, S. Lebedeff, R. Ruedy and L. Travis, 1983: Efficient three dimensional global models for climate studies: Models I and II. *Mon. Wea. Rev.*, **111**, (in press).

Held, I. M., 1978: The vertical scale of an unstable baroclinic wave and its importance for eddy heast flux parameterization. *J. Atmos. Sci.* **35**, 572–576.

——, and A. Y. Hou, 1980: Nonlinear axially symmetric circulations in a nearly inviscid atmosphere. *J. Atmos. Sci.*, **37**, 515–533.

Hide, R., 1977: Experiments with rotating fluids. *Quart. J. Roy. Meteor. Soc.*, **103**, 1–28.

Holton, J. R., 1979: *An Introduction to Dynamic Meteorology.* Academic Press, 391 pp.

Hunt, B. G., 1973: Zonally symmetric global general circulation models with and without the hydrologic cycle. *Tellus,* **25**, 337–354.

——, 1979: The influence of the Earth's rotation rate on the general circulation of the atmosphere. *J. Atmos. Sci.*, **36**, 1392–1408.

Kalnay de Rivas, 1973: Numerical models of the circulation of the atmosphere of Venus. *J. Atmos. Sci.*, **31**, 763–779.

——, 1975: Further numerical calculations of the circulation of the atmosphere of Venus. *J. Atmos. Sci.*, **32**, 1017–1024.

Knollenberg, R., L. Travis, M. Tomasko, P. Smith, B. Ragent, L. Esposito, D. McCleese, J. Martonchik and R. Beer, 1980: The clouds of Venus: A synthesis report. *J. Geophys. Res.*, **85**, 8059–8081.

Kuo, H-L., 1949: Dynamic instability of two-dimensional and nondivergent flow in a barotropic atmosphere. *J. Meteor.*, **6**, 105–122.

——, 1953: On the production of mean zonal currents in the atmosphere by large disturbances. *Tellus,* **5**, 344–362.

——, 1978: A two-layer model study of the combined barotropic and baroclinic instability in the tropics. *J. Atmos. Sci.*, **35**, 1840–1860.

Lorenz, E. N., 1967: *The Nature and Theory of the General Circulation of the Atmosphere.* WMO, 161 pp.

Manabe, S., and J. D. Mahlman, 1976: Simulation of seasonal and interhemispheric variations in the stratospheric circulation. *J. Atmos. Sci.*, **33**, 2185–2217.

——, J. Smagorinsky and R. F. Strickler, 1965: Simulated climatology of a general circulation model with a hydrological cycle. *Mon. Wea. Rev.*, **93**, 769–798.

Marov, M. Ya., 1978: Results of Venus missions. *Annual Review of Astronomy and Astrophysics,* Vol. 16, Annual Reviews, Inc., 141–169.

Miyakoda, K., and J. Sirutis, 1977: Comparative integrations of global models with various parameterized processes of subgrid-scale vertical transports: Description of the parameterizations. *Beitr. Phys. Atmos.*, **50**, 445–487.

Moura, A. D., and P. H. Stone, 1976: The effects of spherical geometry on baroclinic instability. *J. Atmos. Sci.*, **33**, 602–616.

Oort, A. H., and E. M. Rasmusson, 1971: *Atmospheric Circulation Statistics.* NOAA Prof. Pap. No. 5, U.S. Dept. of Commerce, 323 pp.

Plumb, R. A., 1979: Eddy fluxes of conserved quantities by small-amplitude waves. *J. Atmos. Sci.*, **36**, 1699–1704.

Pollack, J. B., 1969: A nongray CO_2-H_2O greenhouse model of Venus. *Icarus,* **10**, 314–341.

——, and R. E. Young, 1975: Calculations of the radiative and dynamical state of the Venus atmosphere. *J. Atmos. Sci.*, **32**, 1025–1037.

——, O. B. Toon and R. Boese, 1980: Greenhouse models of Venus' high surface temperature, as constrained by Pioneer Venus measurements. *J. Geophys. Res.*, **85**, 8223–8231.

Rossow, W. B., 1978: Cloud microphysics: Analysis of the clouds of Earth, Venus, Mars, and Jupiter. *Icarus,* **36**, 1–50.

——, and G. P. Williams, 1979: Large-scale motion in the Venus stratosphere. *J. Atmos. Sci.*, **36**, 377–389.

——, S. B. Fels and P. H. Stone, 1979: Comments on "A three-dimensional model of dynamical processes in the Venus atmosphere." *J. Atmos. Sci.*, **37**, 250–252.

——, A. D. Del Genio, S. S. Limaye, L. D. Travis and P. H. Stone, 1980: Cloud morphology and motions from Pioneer Venus images. *J. Geophys. Res.*,**85**, 8107–8128.

Sagan, C., 1962: Structure of the lower atmosphere of Venus. *Icarus,* **1,** 151–169.

Schneider, E. K., and R. S. Lindzen, 1977: Axially symmetric steady-state models of the basic state for instability and climate studies. Part I: Linearized calculations. *J. Atmos. Sci.,* **34,** 263–279.

Schubert, G., and J. Whitehead, 1969: Moving flame experiment with liquid mercury: Possible implications for the Venus atmosphere. *Science,* **163,** 71–72.

——, C. Covey, A. Del Genio, L. S. Elson, G. Keating, A. Seiff, R. E. Young, J. Apt, C. C. Counselman, A. J. Kliore, S. S. Limaye, H. E. Revercomb, L. A. Sromovsky, V. E. Suomi, F. Taylor, R. Woo and U. von Zahn, 1980: Structure and circulation of the Venus atmosphere. *J. Geophys. Res.,* **85,** 8007–8025.

Seiff, A., D. B. Kirk, R. E. Young, R. C. Blanchard, J. T. Findlay, G. M. Kelly and S. C. Sommer, 1980: Measurements of thermal structure and thermal contrasts in the atmosphere of Venus and related dynamical observations: Results from the four Pioneer Venus probes. *J. Geophys. Res.,* **85,** 7903–7933.

Simmons, A. J., and B. J. Hoskins, 1978: The life cycles of some nonlinear baroclinic waves. *J. Atmos. Sci.,* **35,** 414–432.

Spence, T. W., and D. Fultz, 1977: Experiments on wave-transition spectra and vacillation in an open rotating cylinder. *J. Atmos. Sci.,* **34,** 1261–1285.

Staley, D. O., 1970: The adiabatic lapse rate in the Venus atmosphere. *J. Atmos. Sci.,* **27,** 219–223.

Stone, P. H., 1974: The structure and circulation of the deep Venus atmosphere. *J. Atmos. Sci.,* **31,** 1681–1690.

——, 1975: The dynamics of the atmosphere of Venus. *J. Atmos. Sci.,* **32,** 1005–1016.

Suomi, V. E., L. A. Sromovsky and H. E. Revercomb, 1980: Net radiation in the atmosphere of Venus: Measurements and interpretation. *J. Geophys. Res.,* **85,** 8200–8218.

Taylor, K. E., 1980: The roles of mean meridional motions and large-scale eddies in zonally averaged circulations. *J. Atmos. Sci.,* **37,** 1–19.

Tomasko, M. G., L. R. Doose, P. H. Smith and A. P. Odell, 1980a: Measurements of the flux of sunlight in the atmosphere of Venus. *J. Geophys. Res.,* **85,** 8167–8186.

——, P. H. Smith, V. E. Suomi, L. A. Sromovsky, H. E. Revercomb, F. W. Taylor, P. J. Martonchik, A. Seiff, R. Boese, J. B. Pollack, A. P. Ingersoll, G. Schubert and C. C. Covey, 1980b: The thermal balance of Venus in light of the Pioneer Venus mission. *J. Geophys. Res.,* **85,** 8187–8199.

Travis, L. D., 1978: Nature of the atmospheric dynamics on Venus from power spectrum analysis of Mariner 10 images. *J. Atmos. Sci.,* **35,** 1584–1595.

Whitehead, J. A., 1972: Observations of rapid mean flow produced in mercury by a moving heater. *Geophys. Fluid Dyn.,* **3,** 161–180.

Williams, G. P., and J. L. Holloway, 1982: The range and unity of planetary circulations. *Nature,* **297,** 295–299.

Young, R. E., and G. Schubert, 1973: Dynamical aspects of the Venus 4-day circulation. *Planet. Space Sci.,* **21,** 1563–1580.

——, G. Schubert and K. E. Torrance, 1972: Nonlinear motions induced by moving thermal waves. *J. Fluid Mech.,* **54,** 163–187.

——, and J. B. Pollack, 1977: A three-dimensional model of dynamical processes in the Venus atmosphere. *J. Atmos. Sci.,* **34,** 1315–1351.

——, and ——, 1979: Reply. *J. Atmos. Sci.,* **37,** 253–255.